Metabolic Impairment Occurs Without Changes in Physical Activity in Volumetric Muscle Loss

A Thesis

SUBMITTED TO THE FACULTY OF THE

UNIVERSITY OF MINNESOTA

BY

Kyle Anton Dalske

IN PARTIAL FULFILLMENT OF THE REQUIREMENTS

FOR THE DEGREE OF

MASTER OF SCIENCE

Advisor: Sarah Greising, Ph.D.

March 2021

Acknowledgements

Committee members: Dr. Li Li Ji, Dr. Manda Keller-Ross, and Dr. Sarah Greising

Manuscript co-authors: Christiana J. Raymond-Pope, Jennifer McFaline-Figueroa, Alec M. Basten, Jarrod A. Call, & Sarah M. Greising

Funding through the Clinical & Rehabilitative Medicine Research Program: W81XWH-18-1-0710 (JAC and SMG) and the National Institutes of Health T32-AR050938 (CJRP). Opinions, interpretations, conclusions and recommendations are those of the authors and are not necessarily endorsed by the Department of Defense or National Institutes of Health.

Work was done using the TissueScope LE slide scanner and the C2 Nikon Confocal microscope at the University of Minnesota - University Imaging Centers.

Abstract

As the primary organ of movement, skeletal muscle requires flexible fuel selection to support varying levels of physical activity. For instance, at low levels of activity and during rest, lipids are the primary source of fuel, while carbohydrates are utilized for higher levels of activity. Physical activity is essential for optimal skeletal muscle health and function, and lack of physical activity is associated with various metabolic impairments, such as metabolic inflexibility, a state where skeletal muscle loses efficiency when transitioning between fuel sources. Over time, metabolic inflexibility increases the risk of developing various metabolic comorbidities, such as obesity, diabetes, and heart disease, among others. Metabolic inflexibility can be ameliorated with physical activity and increasing physical activity, however various conditions may impair skeletal muscle and increase the likelihood of inactivity. Orthopaedic injury is an example of a condition that has been shown to reduce physical activity, both acutely and chronically, increasing the risk of metabolic inflexibility and metabolic disorder. Volumetric muscle loss (VML) injury, in which muscle is abruptly lost through traumatic or surgical events, is one such orthopaedic trauma. It is likely that reductions in physical activity and whole-body metabolic impairments occur following VML, however, physical activity and whole-body metabolic outcomes are currently not characterized in the literature. To address this lack of knowledge, a study was designed to evaluate physical activity and whole-body metabolic function at 4 and 8 weeks post-VML injury. The principal finding was that metabolic inflexibility developed independently of changes in physical activity levels following VML injury and that underlying pathophysiologic changes to the muscle may contribute to maladaptive changes at the whole-body level. These findings support that VML injury may increase the risk of metabolic comorbidities, and that future efforts may need to mitigate metabolic maladaptation alongside regenerative and rehabilitative endeavors.

Table of Contents

List of Tables

List of Figures

Abbreviations

ANOVA	Analysis of variance
ATP	Adenosine Triphosphate
AUC	Area under the curve
CLAMS	Comprehensive Lab Animal Monitoring System
CoA	Coenzyme A
CSA	Cross-sectional area
CV	Calorific value
DAMPS	Damage-associated molecular patterns
ECM	Extracellular matrix
ETC	Electron transport chain
$FADH_2$	Flavin adenine dinucleotide
GLUT-1	Glucose transporter 1
GLUT-4	Glucose transporter 4
mRNA	Messenger ribonucleic acid
mTOR	Mammalian target of rapamycin
MyHC	Myosin heavy chain
NADH	Nicotinamide adenine dinucleotide
PGC1-α	Peroxisome proliferator-activated receptor gamma coactivator 1-alpha
ROI	Regions of interest
RER	Respiratory exchange ratio
ROS	Reactive oxidant species

SDH	Succinate dehydrogenase
SERCA	Sarco/endoplasmic reticulum Ca2+-ATPase
SNAP	Soluble NSF attachment proteins
SNARE	Soluble NSF attachment protein receptor
T-tubule	Transverse tubule
VML	Volumetric muscle loss

Chapter 1: Review of the Literature

Basic Skeletal Muscle Structure and Function

Skeletal muscle makes up approximately 40% of the mass of the human body in lean individuals and plays a major role in movement and metabolism [1]. The primary function of skeletal muscle is to produce force, allowing the human body to interact with the outside world. Importantly, skeletal muscle requires energy to function, which necessitates coordination between multiple systems, including the digestive and circulatory systems, to deliver energy-yielding substrates and remove metabolic wastes. Energy utilization in skeletal muscle also generates heat, establishing an additional important role of skeletal muscle in thermoregulation. Knowledge of skeletal muscle has developed over millennia, with an initial focus on basic anatomy and function.

Understanding of human anatomy has continually improved since the times of Galen, DaVinci, and Henry Gray, and a greater understanding of structure leads to a better understanding of function. Skeletal muscles are connected to bones by tendons forming a series-elastic component. The point of attachment that does not move during contraction is the origin, and the point of attachment that moves during contraction is the insertion. Typically, the origin is proximal, and the insertion is distal. Under direction from the nervous system, skeletal muscles contract and apply force on bone within a line of force from insertion to origin. Skeletal muscles control movement through contraction, allowing the origin and insertion points to move closer together, farther apart, or remain at a constant distance. Multiple skeletal muscles typically contract in conjunction, generating movement and stability in multiple planes of motion. Dynamic movement requires coordinated efforts between agonist and antagonist muscles, where agonistic muscles cause a movement through their activation while antagonistic muscles inhibit a movement. Additionally, skeletal muscle contraction is essential for breathing, vision, speech, postural support, and heat production.

To perform various functions, skeletal muscles have a specific anatomical arrangement. A layer of connective tissue called epimysium sheaths skeletal muscle at the most superficial level. Within the epimysium are bundles called

fascicles that are covered by connective tissue layer, the perimysium. Within each fascicle are multiple skeletal muscle cells which are surrounded by the connective tissue, the endomysium. Skeletal muscle cells are referred to as muscle fibers (or myofibers) due to their long, threadlike appearance and will be referred to as such henceforth. Skeletal muscle fibers are long and tubular, with diameters that range in the tens to hundreds of microns, and lengths up to tens of centimeters depending on the organism [2,3]. Muscle fibers are surrounded by the sarcolemma, a phospholipid bilayer with electroconductive properties. Incorporated within and around the sarcolemma is the extracellular matrix (ECM), made up largely of collagens and proteoglycans [4]. The ECM is important for both structure and function, contributing to force generation and cell signaling [4].

Deep to the ECM are skeletal muscle fibers, the main cells of contraction. Skeletal muscle fibers are composed of highly organized functional units called sarcomeres, which are aligned in series longitudinally and give the muscle a striated appearance. Sarcomeres are made up of the contractile proteins (i.e., myosin and actin), structural proteins (e.g., titin and actinin), and regulatory proteins (e.g., troponin and tropomyosin) [5]. In the presence of ionic calcium and at the expense of energy in the form of adenosine triphosphate (ATP), myosin reversibly binds with actin, forming a cross-bridge. Myosin uses energy and performs a power stroke, pulling actin and generating force towards the midline, then myosin detaches, resets, binds to a new actin, and performs another power stroke [5]. This cycle, termed the cross-bridge cycle, repeats and occurs along the entire length of skeletal muscle fibers and throughout the entire muscle, resulting in whole muscle contraction and force generation. Cross-bridge cycling of myosin on actin allows sarcomeres to shorten (isotonic contraction), lengthen (eccentric contraction), or remain the same length (isometric contraction) in response to an external force [6].

Key Supporting Cells and Organelles

All tissues in the body undergo development, growth, and repair which is typically accomplished by mitosis (hyperplasia) or cell growth (hypertrophy) of existing cells, and differentiation of stem cells. However, mature skeletal muscle in humans is post-mitotic; therefore, muscle fiber turnover rate is approximately zero during normal maintenance [7]. Instead of undergoing mitosis, skeletal muscle fibers are equipped with up to hundreds of nuclei per myofiber [8] that provide the transcriptional information to replace and maintain fiber components. Nuclei in a skeletal muscle fiber are dispersed throughout the cell, and each nuclei regulates gene expression in its own localized cytoplasmic region of the cell, termed the myonuclear domain [3,9]. In response to various stimuli, nuclei number and activity can be altered, allowing the muscle fiber to dynamically change its metabolic properties [9]. Total transcriptional and translational trends in a skeletal muscle fiber are reflections of the coordinated activity of all of the myonuclear domains within the cell. Therefore, if muscle growth is to occur, it must be achieved by modulating the activity or number of myonuclear domains.

Stem and Pericyte Cells

In response to skeletal muscle injury, muscle fibers acquire new nuclei via the fusion of satellite cells, which are undifferentiated, local, myogenic progenitor cells [2]. Satellite cells are separate from the muscle fiber and located between the basal lamina and the sarcolemma [2], and remain in a quiescent state until activated by myogenic regulatory factors [10]. While mature skeletal muscle cells are post-mitotic and largely incapable of division, satellite cells are capable of dividing and thus capable of providing new nuclei to muscle fibers. Satellite cells either divide symmetrically, generating two new stem cells to expand the satellite cell pool, or asymmetrically, generating one stem cell to maintain the satellite cell pool and one myogenic cell that will terminally differentiate [11].

Maintaining a pool of satellite cells is critical to allowing skeletal muscle to respond to circumstances that require the accretion of new nuclei. Expanding the

myonuclear domain by satellite cell mediated nuclear addition increases the capacity for protein synthesis, allowing muscle fibers to increase in size and maintain size increases. In an experimental setting, skeletal muscle growth can occur independent of myonuclear addition [12], but ultimately, significant muscle growth and maintenance of muscle growth *in vivo* requires expansion of the myonuclear domain by adding nuclei to the muscle fiber, typically utilizing satellite cells [13,14].

Satellite cells are required for skeletal muscle regeneration, however other cells are capable of contributing nuclei under certain circumstances. Throughout the body, there are cells that can fulfill multiple roles, a characteristic that is essential for growth, development, and maintenance of tissues. For example, pericytes are cells that are capable of differentiating into adipocytes, chondrocytes, osteocytes, phagocytes, granulocytes, and myocytes depending on their environment [15,16]. Pericytes are found ubiquitously throughout the human body, colocalized with microvasculature. While the most understood role of pericytes is in controlling angiogenesis, many different roles of pericytes have been identified. In recent decades, pericytes have been implicated in regulating a variety of physiologic functions, such as: blood flow, blood vessel permeability, innate immune response, and collagen deposition, among others depending on external stimulus [15].

The multipotent differentiation potential of pericytes is dependent upon their environment. In an experiment conducted by König et al., pericytes that were isolated from murine adipose tissue and seeded on an artificial bone scaffold differentiated into osteoblasts, promoting bone union following a surgically induced fracture [17]. In skeletal muscle, pericytes fulfill their primary function in controlling angiogenesis, but also exhibit myogenic potential. Dellavalle and colleagues traced the lineage and differentiation of pericytes and found that they are capable of contributing to the satellite cell pool and subsequently contributing to growth and regeneration of skeletal muscle [18]. All in all, pericytes are a key cell that lends to the dynamic nature of skeletal muscle.

Organelles

Postnatal skeletal muscle growth in mammals is primarily accomplished through muscle hypertrophy [19]. While expanding myonuclear domains is necessary for muscle growth, it is ultimately the upregulation of ribosomes that facilitates muscle hypertrophy. Ribosomes are the key organelles of protein synthesis throughout the body, including in skeletal muscle. They generate various proteins within muscle fibers by translating mRNA that originates from the nuclei within the fiber. After a growth-promoting stimulus such as from resistance exercise, factors like the mammalian target of rapamycin (mTOR) are upregulated, promoting ribosomal biogenesis [19]. By increasing the total number of ribosomes, translational capacity increases, allowing the muscle fiber to expand in size. Just as ribosomes are a key organelle of protein synthesis, mitochondria are key organelles of energy metabolism.

Mitochondria are found within nearly all cells in the body, including skeletal muscle. Initially of bacterial origin, mitochondria have evolved in a symbiotic manner with eukaryotes [20], contributing to and performing many essential functions throughout the body. The major and most well-known role of mitochondria is in oxidative metabolism, where glucose is completely oxidized and broken down to generate energy through aerobic respiration, using a process known as the Krebs cycle (also known as the citric acid cycle or tricarboxylic acid cycle). Importantly, enzymes for the Krebs cycle are only found within the mitochondria, therefore aerobic respiration occurs exclusively in mitochondria. Additionally, mitochondria are involved with regulating cell proliferation, apoptosis, redox balance, intracellular calcium, heat production, among other functions [21].

To perform their various functions, mitochondria are regulated and arranged in a highly controlled manner. In skeletal muscle, mitochondria form a highly organized and dynamic matrix that adjusts based on the metabolic needs of the muscle. Depending on stimuli from signaling molecules, such as peroxisome proliferator-activated receptor gamma coactivator 1-alpha (PGC-1α), mitochondria are capable of undergoing biogenesis, fission, and fusion to respond to metabolic

need by altering quantity and quality of mitochondria [22,23]. For example, endurance exercise increases expression of PGC-1α, which consequently promotes mitochondrial biogenesis, expanding the mitochondrial network [24]. Expanding the mitochondrial network within skeletal muscle in such a way improves the capability of the muscle to utilize glucose and fatty acids as energy-yielding substrates, thus improving whole muscle metabolic capacity.

While skeletal muscles are similar in their general structure and function, variations between key cells and organelles within muscle fibers result in differences in functional characteristics of the overall muscle. These variations in characteristics allow different muscles to be categorized by their phenotypic qualities, which will be discussed in the subsequent section.

Characterization of Skeletal Muscle

Evidence has existed for over half a century that motor neurons drive skeletal muscle fiber characteristics. In a key study, when Buller and colleagues severed the nerves from feline soleus muscles and cross innervated the soleus muscle with nerves from the flexor digitorum longus muscles, the soleus took on properties that resembled the flexor digitorum longus. The reverse occurred in the flexor digitorum longus muscle, which expressed characteristics of the soleus muscle [25]. Burke and Edgarton expanded on the principle that the motor neuron derives fiber type and classified motor units based on muscle fiber contractile speed (fast or slow twitch) and fatigue resilience of the motor unit [26]. Collectively, motor units are characterized as slow-twitch fatigue resistant (Type S), fast-twitch fatigue resistant (Type FR), fast-twitch fatigue intermediate (Type FInt), and fast-twitch fatigable (Type FF). General characteristics of certain types of muscle fibers are outlined in **Table 1**.

Table 1. Muscle Fiber Characteristics				
Motor Unit Type	**Type S, slow-twitch**	**Fast, fatigue-resistant**	**Fast, fatigue-intermediate**	**Fast, fatigable**
Muscle fiber type	Type I	Type IIa	Type IIx	Type IIb
Innervation ratio	Low	Moderate	Moderate	High
Myosin heavy chain (MyHC) isoform	$MyHC_{slow}$	$MyHC_{2A}$	$MyHC_{2x}$	$MyHC_{2b}$
Muscle fiber cross section diameter	Small	Intermediate	Large	Very Large
Contraction speed	Slow	Moderately Fast	Fast	Very Fast
Fatigue resistance	High	Fairly High	Intermediate	Low
Capillary supply	High	Intermediate	Low	Low
Mitochondrial content	High	High	Intermediate	Low
Glycolytic enzyme content	Low	Intermediate	High	High
Myosin heavy chain (MyHC)				

Characteristics of Skeletal Muscle Fiber Types

Muscle fibers within a specific motor unit express isoforms of myosin heavy chain (MyHC) that reflect the functional properties of the associated muscle fiber. For example, a skeletal muscle fiber within a Type S motor unit contracts slowly, therefore, it will express $MyHC_{slow}$, a form of myosin that has slower contractile speed. Muscles fibers within Type FR motor units contract faster than those of Type S motor units, and express $MyHC_{2A}$. Type FInt motor unit muscle fibers express $MyHC_{2x}$, allowing contractile speeds greater than Type S and FR motor units. Lastly, muscle fibers of Type FF motor unit express $MyHC_{2b,}$ which allows contractions slightly faster than all other muscle fiber types. Muscle fibers are commonly typed by MyHC isoform expression, where fibers that express primarily $MyHC_{slow}$ are classified as type I, $MyHC_{2A}$ are type IIa, $MyHC_{2x}$ are type IIx, and $MyHC_{2b}$ are type IIb, which are notably only found in rodents [27]. While many fibers express single MyHC isoforms, co-expression of muscle fiber types occurs. For example, in a study by Bottinelli et al., co-expression of fast myosin isoforms occurred in 50% of plantaris fibers and 30% of tibialis anterior fibers in rats [28],

and Billeter et al. observed hybridization of type IIa and IIb fibers, and various hybridizations of type I muscle fibers [29]. Hybridization is more likely during embryonic development and during pathological states, and often involves types I/IIa, and IIx/IIb [30].

When considering muscle fiber classification, it is also important to understand how metabolism varies between various muscle fiber types. In general, oxidative metabolism is utilized for long term energy generation, whereas glycolytic metabolism is utilized for fast contractile activity [26]. As a slow contracting and fatigue resistant muscle fiber type, type I muscle fibers rely primarily on oxidative metabolism. Type IIa muscle fibers have faster contractile activity than type I and are somewhat fatigue resistant and thus utilize a combination of oxidative and glycolytic metabolism. As a fast twitch and fatigue intermediate fiber, type 2x fibers primarily utilize glycolytic metabolism, but maintain some capability for oxidative metabolism. As the fastest contracting muscle fiber type, type IIb fibers rely almost entirely on glycolytic metabolism.

Whole Skeletal Muscle

Characteristics of whole skeletal muscle are determined by the overall composition of muscle fibers in that muscle. In humans, a muscle that is fatigue resistance (i.e., predominately slow-twitch) is typically composed of a high proportion of type I muscle fibers whereas muscles that are highly fatigable have a higher proportion of type II muscle fibers [31]. For example, muscles that are used throughout the day for walking and posture, such as the soleus muscle, are composed primarily type I fibers [32]. In contrast, muscles such as the vastus lateralis muscle are used to generate large force during a jump or squat, and have a higher proportion of type II fibers [33]. While some muscles may have a higher proportion of specific fiber types, it is important to note that most muscles have a distribution of fibers with a spectrum of fiber types [33].

Skeletal Muscle Contraction and Activation

The somatic branch of the nervous system voluntarily controls skeletal muscles. Regions of the brain including the cerebrum and cerebellum send signals to upper motor neurons (contained in the brain and brainstem), which relay signals to the lower motor neurons [34]. Lower motor neurons that innervate skeletal muscles are alpha motor neurons. Axons of alpha motor neurons terminate on skeletal muscle fibers at the motor end plate, a specialized synaptic region on the skeletal muscle fiber. The connection between an alpha motor neuron and the skeletal muscle fiber it innervates is the neuromuscular junction.

Individual muscle fibers are innervated by a single motor neuron at the neuromuscular junction, but a single motor neuron may form a unit with less than ten or up to thousands of muscle fibers [35,36]. The motor neuron and all muscle fibers it innervates is called a motor unit. All muscle fibers in a motor unit will exhibit qualities as dictated by the type of motor neuron, as previously discussed. The variance in fiber number per motor unit is the innervation ratio; a motor neuron with a large innervation ratio innervates more muscle fibers than a motor neuron with a smaller innervation ratio [37–39]. Motor units with small innervation ratios are utilized for movements that require finer control (e.g., writing or eye movement) whereas motor units with large innervation ratios are utilized for gross movements (e.g., knee extension or elbow flexion). Whole muscle contraction is a net result of coordinated motor unit activity. Motor units are recruited as needed by the size principle [40], starting with smaller type S motor units for weaker, highly controlled, and sustainable contractions, followed with larger type FF motor units as the need for force generation increases.

Excitation Contraction Coupling

The coupling of excitation and contraction in skeletal muscle results from a series of specific electrochemical events. When a motor neuron is stimulated to threshold, an action potential is transmitted from the motor neuron to the motor end plate. A graded potential is then generated at the motor end plate, which

initiates action potentials bidirectionally down the muscle fiber, eventually reaching a structure called the transverse tubule (t-tubule). The t-tubule is a specialized portion of the sarcolemma that allows action potentials to go deep within the muscle, initiating calcium release from the adjacently located sarcoplasmic reticulum [41]. Calcium is very concentrated within the sarcoplasmic reticulum and once release is initiated, calcium travels down its concentration gradient and floods the sarcoplasm of the muscle fiber, initiating subsequent stages of muscle contraction.

Calcium that is released from the sarcoplasmic reticulum binds to troponin, a regulatory protein that associates with actin and tropomyosin [41]. Calcium-bound-troponin moves tropomyosin to expose the myosin-binding site on actin. Once the myosin binding site is exposed and providing there is adequate ATP, myosin is free to bind with actin and perform a power stroke and force generation of myosin on actin [41]. Calcium ATPase pumps (SERCA) located on the sarcoplasmic reticulum transport calcium from the sarcoplasm to the sarcoplasmic reticulum, preventing a cytotoxic response and prolonged contraction of the muscle fiber. Relaxation of the muscle fiber follows once intracellular calcium concentrations are sufficiently reduced by SERCA-mediated removal.

Skeletal Muscle Metabolism

Normally, skeletal muscle maintains a homeostatic balance of protein catabolism and anabolism, both of which require energy [42]. In general, muscle hypertrophy is a state where anabolism is greater than catabolism, and atrophy is a state where catabolism outpaces anabolism. Protein homeostasis is dynamic and complicated and fluctuates depending on various factors related to energy intake and stimulus from movement. For example, during exercise, muscle catabolism is greater than anabolism, resulting in the breakdown of skeletal muscle [43]. However, stimulus from exercise subsequently promotes protein anabolism, which either rebuilds the muscle to its original state, or results in hypertrophy beyond the pre-exercise state [43]. Skeletal muscle is capable of utilizing protein,

carbohydrates, and lipids for energy. Amino acids from proteins are essential for building and maintaining muscle, however amino acids are used primarily as material for building proteins rather than as energy substrates [44]. Therefore, glucose and lipids are the main energy-yielding molecules in skeletal muscle.

In skeletal muscle, glucose is a central molecule in both glycolytic and oxidative metabolism. Glucose is transported into the muscle from the blood and is either used immediately for generating energy in the form of ATP or is stored as glycogen (or eventually fat) for future use [45]. The fate of glucose is determined by the current state of the muscle. At rest, glucose is primarily stored, since there is no immediate need to generate large amounts of energy. During exercise, glucose is used both from local glycogen stores and from the blood, however glucose enters the muscle utilizing a different transporter during exercise compared to at rest. Resting skeletal muscle uses glucose transporter 1 (GLUT1) to transport glucose across the membrane in a process that is mediated by insulin signaling [45]. During exercise, glucose transporter 4 (GLUT4) is the primary glucose transporter in skeletal muscle and is translocated to the sarcolemma from intracellular vesicles, dramatically increasing glucose uptake capacity [45]. It is believed that contraction is the primary driver of GLUT4 translocation, however the mechanism is not clearly understood. It is theorized that depolarizing calcium plays a large role in GLUT4 translocation, possibly through mediating activation of the SNARE complex, a group of proteins involved in vesicle transport [46]. Mobilization of GLUT4 in this manner is also dependent on the actin cytoskeleton, which is located right beneath the sarcolemma. It is through coordination of markers and receptors on the actin cytoskeleton and the vesicles containing GLUT4 that GLUT4 is translocated to the proper location. Therefore, it is essential that muscle membrane integrity is maintained, and perturbations to membrane structure and contractile function—as during injury, disease, and illness—may impair glucose transport.

Once glucose has entered a muscle cell, glycolysis may begin. During glycolysis, glucose is cleaved to liberate energy and produce pyruvate, and ultimately lactic acid. Glycolysis is an anaerobic process and is only viable for short

term, rapid energy production since the energy produced per glucose molecule is low, and lactic acid build up is toxic [47]. Alternatively, after pyruvate is produced from glycolysis it can be converted into acetyl-CoA and transported into mitochondria. Once inside of mitochondria, acetyl-CoA can enter the Krebs cycle, a process where acetyl-CoA undergoes various enzymatic conversions, producing energy-yielding intermediates (e.g., NADH and $FADH_2$) and carbon dioxide [48]. Energy-yielding intermediates from the Krebs cycle are then utilized in the electron transport chain (ETC), which is a complex of proteins located in the mitochondria where NADH and $FADH_2$ are used in conjunction with oxygen to produce ATP and water [48]. In sum, the Krebs cycle and ETC comprise oxidative metabolism, where all of the carbon molecules in glucose are completely oxidized for the purpose of ATP generation. Oxidative metabolism produces much more ATP per glucose molecule, but is a slower process than glycolysis, so it is much better suited for providing energy long term.

In many respects, lipids in muscle metabolism parallels glucose utilization, however there are some key differences. Lipids contain long carbon chains that can be cleaved off and converted to many acetyl-CoA molecules for use in the Krebs cycle. The carbon chains in lipids vary in length, but generally have many more carbons than a glucose molecule. Therefore, fats are an efficient way to store energy and can produce substantially more energy per molecule than glucose. Similar to glucose, lipids are transported from the blood to the inside of the muscle fiber where eventually carbons are cleaved for use in the Krebs cycle and ETC. If muscle energy balance is positive (i.e., there is sufficient available energy from glucose), or when the muscle is at rest, lipids are stored within the muscle fiber as intra-myocellular lipids rather than oxidized [49]. Lipids that are stored in the muscle cell can be beneficial, as they serve as a local energy store. This is apparent in endurance athletes, who have more lipid droplets in their muscles than untrained individuals [49]. Lipid dynamics are challenging to study since rodents do not store lipids within their muscles as readily as humans do, however, researchers have identified various negative consequences of lipid oversupply in

skeletal muscle. Perhaps most notably, excess lipids can result in lipotoxicity, where lipid derivatives impair regular cellular processes [49]. Lipotoxicity has been coined as the primary cause of insulin resistance and subsequent development of type 2 diabetes and has been implicated as a factor that contributes to worsening sarcopenia, impaired mitochondrial quality, and reduced GLUT4 translocation.

Skeletal Muscle Damage and Repair

Skeletal muscle is capable of completely repairing itself following a variety of injuries. The repair process includes removing damaged tissue, repairing damaged fibers, and the accretion of new nuclei in fibers that have lost nuclei as a result of damage. After a muscle is injured, neutrophils infiltrate the cite of injury, begin clearing debris and any foreign material from the site of injury, and release chemoattractant factors [50]. Soon after, macrophages are recruited and accumulate. Initially, M1 macrophages promote further inflammation and phagocytosis [51]. Once M1 macrophage activity begins to decline, M2 macrophages take over and secrete anti-inflammatory cytokines and signaling factors that promote tissue regeneration [51]. A key aspect of skeletal muscle regeneration is the activation and proliferation of satellite cells. When activated, satellite cells rapidly divide and subsequently give rise to myogenic progenitors [52]. Some of the myogenic progenitors will differentiate and form myofibers to regenerate damaged muscle fibers, while the remaining progenitors repopulate the satellite cell pool [52]. The muscle is considered regenerated once all damaged muscle fibers are repaired and the muscle's ability to generate force is restored, allowing functionality equal to the pre-injured state. However, complete and successful regeneration does not always occur, such as the cases when volumetric muscle loss (VML) injury occurs. To better understand the complicated aspects of regeneration in skeletal muscle, it is prudent to consider various modes of skeletal muscle injury and disease.

Toxin and Burn Injury

One model of skeletal muscle injury and recovery is toxin injury [53]. Essentially, various myopathic toxins, such as notexin, cardiotoxin, or α-bungarotoxin are injected, damaging the muscle and other surrounding tissue, then regeneration is studied over time [54]. Notexin is a venom that destroys the sarcolemma of muscle fibers, resulting in a toxic calcium influx and subsequent necrosis [55]. Another commonly used venom, cardiotoxin, similarly targets plasma membranes and results in calcium induced necrosis. Rather than by direct degradation of membranes, cardiotoxins form pores in membranes, resulting in a toxic influx of calcium [56]. Notexin and cardiotoxin injury results in substantial damage to skeletal muscle, but complete regeneration and restoration of function is possible within approximately four weeks [55,57]. Other toxins may result in permanent damage, α-bungarotoxin targets and destroys receptors for acetyl choline, irreversibly preventing end plate potentials from occurring [58]. While the contractile proteins are not damaged from α-bungarotoxin, functionality of the muscle is severely impeded due to uncoupling excitation and contraction.

Toxin injury is a valuable example of an often-used injury model to evaluate recovery, or lack of recovery, of skeletal muscle, however there are various other injury and disease states that add layers of complexity to studying and treating skeletal muscle injury. Thermal injuries are an example of an acute injury to skeletal muscle. Burns from fire, scalding, or alternative heat sources can cause both superficial and deep damage to tissues, resulting in various structural and metabolic perturbations. If a burn is severe enough to damage skeletal muscle, the effected tissues will have an instantaneous local and systemic response. Initially, pro-inflammatory cytokines are released, and the organism enters a state of shock, where metabolic rate is slowed, heart rate decreases, and cardiac output is reduced [59]. After a few days, a hypermetabolic state is initiated as the organism is flooded with endogenous catecholamines and corticosteroids, resulting in a dramatic increase in metabolic rate, heart rate, and body temperature [59].

Importantly, the more severe the burn, the greater the metabolic disturbance after the burn [60,61].

Though a burn injury occurs acutely, there are various chronic consequences. For example, the robust inflammatory response may take up to half a year to abate, and the hypermetabolic response may never return to a preinjury state [59]. The aspects driving this hypermetabolic state are largely related to the energy expense of healing, as well as a conversion of skeletal muscle to a thermogenic phenotype. In a murine burn experiment conducted by Porter et al., experimenters found that skeletal muscle experiences an uncoupling of mitochondrial function following burn injury [62]. In other words, oxidative metabolism was severely impaired while thermogenesis was promoted. Interestingly, muscles that were both local and distal to the site of the burn experienced mitochondrial uncoupling, albeit with a less extreme response distally. Traumatic injury often has system wide impairments, and burn injury aligns with that trend. The post-burn environment promotes full body catabolism, protein degradation, insulin resistance, muscle wasting, and multi-organ dysfunction [59]. Preserving skeletal muscle through exercise (e.g., rehabilitation), hormone supplementation, and dietary supplementation, has been found to improve morbidity and mortality in burn victims, supporting that skeletal muscle is a key player in the health and function following burn injury [63].

Denervation

When a skeletal muscle loses neural connections, whether by severing of nerves or destruction of neuromuscular junctions, the muscle fiber is considered denervated. Depending on the severity of the injury, a whole skeletal muscle may be completely denervated or partially denervated. With denervation comes corresponding functional loss. In other words, if a skeletal muscle is completely denervated it will lose all endogenous ability to generate force, while if some neural connections are maintained, some capacity for force generation will remain. Due to the removal of neural stimulus and lack of activity, abrupt and severe atrophy is

inevitable in denervated skeletal muscle. Significant atrophy is observable within days following denervation and continues to worsen over time, with some muscles atrophying to less than half of their original size [64,65].

Many aspects of muscle metabolism are altered by denervation beyond atrophy. Notably, skeletal muscles that have lost innervation lose glycolytic muscle fibers and shift towards a more oxidative phenotype [64]. Despite the selective preservation of oxidative muscle, mitochondria are dysregulated following denervation, leading to impaired oxidative metabolism. Specifically, mitochondrial fraction by muscle mass decreases, apoptotic signaling increases, reactive oxidant species (ROS) production increases, ATP production is reduced, and the mitochondrial fission and fusion is disrupted [66–68]. All of these factors contribute to poor functional outcomes, even in the event that the nervous connection is reestablished [69].

Critical Illness

When critical illnesses occur, such as secondary to heart failure, cancer, respiratory distress, and organ failure, the body enters a state of survival. In such a state, maintaining the muscular system is not a priority. In fact, the muscular system tends to waste, as was observed in a prospective study conducted by Lodeserto and Yende, where critically ill patients were found to lose ~10% of their rectus femoris size in 10 days [70]. Besides sheer size loss, critically ill patients had reduced muscle fiber cross sectional area and reduced protein synthesis, and 54% of patients had myofibers necrosis. The phenomenon where muscle is rapidly lost during critical illness has been under investigation for over a century. In the last 50 years, Bolten et. al coined the term “critical illness polyneuropathy”, linking the muscle wasting to sepsis [71]. Typically, critical illness polyneuropathy is paired with myopathy, both of which affect more than one third of critically ill patients [72]. While maintaining skeletal muscle may not be critical in acute moments when life is in the balance, it does play a substantial role in long-term survival, health, and function once the initial crisis has resolved.

While not all critical illnesses effect skeletal muscle in exactly the same ways, there are a few common consequences following critical illness. In general, the body enters a state that promotes catabolism, resulting in significant weight loss and atrophy of skeletal muscle tissue, especially type II fibers [72–74]. During critical illnesses secondary to heart failure and cancer, cachexia can occur, a multifactorial syndrome characterized by progressive full-body wasting [75]. Cachexia is severe and often irreversible, even with sufficient dietary intake and supplementation, and since it is poorly understood, the recommended way to treat cachexia is to treat the primary illness. This is problematic because critical illnesses are often difficult to treat and requires long term, individualized care. Further, metabolism during critical illness is dysregulated beyond heightened catabolism. Mitochondria are especially sensitive to critical illness, and dysregulation of the mitochondrial network is expected to contribute to other aspects of critical illness that affect skeletal muscle, such as cachexia, increased oxidative stress, and lower oxidative capacity [72,76].

Whatever the etiology of critical illness, skeletal muscle is typically negatively affected. Whether directly by the pathophysiology of the condition, or indirectly by inducing low mobility and physical activity, it is important to consider skeletal muscle health when establishing an effective treatment plan. In the past few decades, evidence suggests that early mobilization improves patient outcomes following critical illness, while lack of mobilization results in prolonged recovery and worse outcomes [72,77].

Muscular Dystrophy

Muscular dystrophies are genetic disorders where mutations in structural proteins, such as dystrophin or titin, can result in muscle and metabolic dysfunction, and early death [78]. There are more than 30 types of muscular dystrophy with different pathologies depending on what proteins are affected. Regardless of the type of dystrophy, the affected muscles are of lower structural and functional quality and have increased susceptibility to necrosis and apoptosis

[79]. Dystrophic muscles attempt to repair and replace damaged or lost muscle fibers, however the endogenous repair is insufficient and further degeneration is expected. Indeed, a hallmark of muscular dystrophy is a cycle of degeneration and regeneration, which typically worsens as the disease progresses [79]. With degeneration and regeneration cyclical, robust inflammation is typical. Unfortunately, inflammation is also a driver of further degeneration, resulting in even further inflammation [79]. The inflammatory and degenerative environment that is established in muscular dystrophy is not favorable for muscle regeneration and instead promotes the development of fibrosis, another hallmark of muscular dystrophy [78,80]. Problems with regulating connective tissue (e.g. fibrosis) is a central issue in muscular dystrophy, which often is linked to problems at the muscle membrane.

Disruptions in muscle membrane function and integrity, as observed in muscular dystrophies, can have severe consequences for whole body metabolism. One critical example is aberrant glucose metabolism. Dystrophic muscle, especially in dystrophies that specifically effect membrane transport proteins, becomes increasingly insulin resistant over time [79]. As muscle continues to break down and fibrosis builds up, the decrease in total amount of muscle tissue involved in insulin-mediated glucose metabolism often results in increased prevalence of diabetes and obesity among dystrophic patients [79]. Such impairments have cyclical consequences, where dystrophy promotes and exacerbates diabetes, and diabetes further impairs the body’s ability to regenerate and balance metabolic needs. Recent works have targeted collagens that may have specific roles in muscular dystrophy symptoms.

Collagen VI, a collagen associated with fibrosis, is increased in dystrophic muscle [81] and it is possible that collagen VI is deposed in excessive amounts and is inhibitory towards muscle function and metabolism. However, the relationship between muscle function and fibrosis is imprecisely understood. In a dystrophic mouse model where collagen VI was ablated, de Greef et al. found that fibrosis decreased, but muscle function did not improve, supporting that some

fibrosis is beneficial [82]. Further, the experimenters found that, while total body mass and activity did not change significantly, there was a significant decrease in lean body mass. All aspects considered, the relationships between metabolism and fibrotic muscle are complicated. The effects of fibrotic deposition, disruption to the muscle, and whole body metabolic impairment may be relatable to outcomes following muscle injuries that result in fibrotic deposition, even though there is a different etiology.

Sedentarism, Bedrest, and Immobilization

The human body evolved to move in order to survive and only functions optimally with adequate physical activity. Without pressures such as hunger and threats to survival, humans in modern society are often inactive and sedentary, which contributes to decreased health and an increase in all-cause mortality [79,80]. Groups that are especially at risk of being sedentary and unfit are people that have suffered past orthopeadic injury [83,85,86].

There are a variety of ways that sedentarism and low physical activity contributes to poor health, including an increase in risk of being overweight or obese and decreased cardiac function [87]. A precursor to many of these maladaptive conditions is the development of metabolic inflexibility, a state where skeletal muscle has reduced sensitivity to insulin-signaled glucose uptake [88]. Since skeletal muscle makes up such a large portion of the human body, dysregulation of glucose metabolism in inactive skeletal muscle contributes strongly to the development of a plethora of disorders and diseases relating to metabolism, such as: type 2 diabetes mellitus, atherosclerosis, heart disease, obesity, non-alcoholic fatty liver disease, and osteoporosis [87].

Even more extreme examples of sedentarism are immobilization and bedrest. Skeletal muscles are especially affected by lack of use during immobilization and bedrest. A study conducted by Irimia and colleagues found dramatic onset of functional deficits during a prolonged period of bedrest [89]. Namely, in the lower limb there was significant muscle atrophy, major decrements in force and power

output, and large decreases in oxidative gene expression. These changes have lasting implications when considering long-term outcomes. Following immobilization, muscles are resistant to rehabilitation and take longer to regain function, largely due to downregulation of PGC-1α [90].

Aging and Sarcopenia

With age comes progressive decline of all systems in the body, including the muscular system [91]. Loss of muscle mass and function with advancing age, is termed sarcopenia. When considering chronic aspects of skeletal muscle injuries and conditions, sarcopenia may be an important comorbidity to consider. For instance, with aging comes persistent inflammation, muscle atrophy, and reduced muscle function [92,93]. It is difficult to delineate all factors surrounding sarcopenia because many factors covary with other aspects of sarcopenia. It is challenging to pinpoint to what degree atrophy occurs directly as a result of muscle aging because other systems that relate to muscle function, such as the circulatory and respiratory systems, also experience age related declines [91]. Further, decline of skeletal muscle, respiratory, and circulatory systems all contribute to the decline of mitochondrial function. However, mitochondrial dysfunction contributes to muscle atrophy [94], establishing a paradoxical situation where it is difficult to determine to what extent mitochondrial dysfunction contributes to muscular system decline, and vice versa. Regardless, it is theorized that loss of mitochondrial control mechanisms has a significant role in the development and propagation of sarcopenia.

As humans age, mitochondrial quality control mechanisms (i.e., fission, fusion, and autophagy) decline [21]. Low quality mitochondria contribute to damage associated molecular patterns (DAMPS), which are the primary link between mitochondria and inflammation. One of the main DAMPs involving mitochondria is an impaired capacity to balance ROS, which eventually leads to mitochondrial lysing. Though mitochondria have formed a symbiotic relationship with eukaryotes, liberated mitochondrial DNA is still recognized as foreign by the immune system,

inciting the recruitment of white blood cells, further promoting inflammation [21]. Inflammation incited in this way is inhibitory to muscle function, and is observed in various types of muscle injury [95]. It may be important to consider how inflammatory cells may interact with muscle function and the health and function of the organism as a whole, especially when considering chronic outcomes following muscle injury.

Volumetric Muscle Loss Injury

In cases of severe orthopaedic trauma, such as from high-energy blast wounds or car accidents, individuals may sustain massive damage to their entire body. Following such trauma, the primary focus is triage. Modern medicine has increased survival rates for these injuries, leaving afflicted individuals with a new set of concerns. Traumatic injuries often have chronic consequences on whole organism function and health. This is especially true in cases of VML injury.

Volumetric muscle loss injury occurs when skeletal muscle is damaged and abruptly removed, resulting in frank loss of skeletal muscle tissue and chronic fore loss [96]. Relatively small losses of muscle tissue (<30%) result in disproportionately severe functional losses anywhere from 30-80% [97,98]. These injuries are beyond the capacity of endogenous repair, resulting in chronic disablement. No therapeutic method allows a full recovery of function of the skeletal muscle. In fact, a recent meta-analysis by Greising and colleagues supports that, while treatment resulted in an approximate 16% improvement, the majority of the initial deficit remained, resulting in a relatively small overall effect when compared to non-injured controls [99]. In human, patients that suffer VML injury may expect poor outcomes despite substantial effort and expense during the course of treatment.

Care for VML injury involves a lengthy time course of medical treatment, including, at a minimum, surgical fees and extensive physical therapy. The estimated cost to treat VML injury for an individual patient is expected to exceed $341,000, resulting in a significant burden to the healthcare system and the patient

[100]. It is difficult to quantify the total incidence of VML injuries since there is no ICD code. Based on the number of traumatic orthopaedic injuries in the armed services and civilian population, there are an expected significant number of VML cases per year [100,101]. Since these cases do not truly resolve, it can be implied that there will be a largely increasing number of patients undergoing treatment for the chronic aspects of VML injury, driving a need to develop a standard of care for these injuries. This is problematic, as the pathophysiology of VML injury is still incompletely understood.

There are a multiple mechanisms to consider when attempting to characterize and understand the complexities underlying VML injury. The causes of VML injury vary, but they are often traumatic or surgical in nature. Following trauma, the focus of initial care is to mitigate vascular injury, infection, and address any bone injury. In this process, tissues at risk for necrosis are debrided, including skeletal muscle. It is unavoidable that such a loss of muscle from damage and debridement will cause an instantaneous loss of function.

With traumatic loss of muscle comes a likely loss of nerve tissue. In a VML injury experiment conducted by Corona et. al, though motor neurons remained, axotomy occurred alongside VML injury [102]. The loss of neuromuscular structures contributes to the loss of function after VML injury in a few ways. Muscle fibers require stimulus from motor neurons to contract, so any loss of innervation will functionally reduce the total number of muscle fibers capable of contracting. Additionally, muscle fibers require innervation to remain viable, any loss of innervation to a muscle fiber will inevitably result in the death of that fiber [99]. Therefore, even if muscle fibers regenerate after VML injury, they will not survive without innervation. Within the complicated interplay of neuromuscular injury and attempted recovery, aspects of healing that are supposed to be beneficial—such as the inflammatory response—become malignant.

Ordinarily the inflammatory response is an essential aspect of recovery following injury, however, the substantial inflammatory response after VML injury is not entirely beneficial. From the initial injury, the inflammatory response is robust

and chronic [97,104]. A lasting inflammatory response promotes an anti-regenerative environment [105] that promotes fibrotic differentiation of progenitor cells [16]. While a recoverable injury will result in the downregulation of the fibrotic response after a few days to weeks, this is not the case in VML injury. Much like in the case of muscular dystrophies, fibrosis permeates the affected muscle. To some extent, the extensive fibrotic response after VML injury may be useful in preserving some degree of function. In a recent study, Corona et al. found that pharmacological mitigation of fibrosis resulted in a lower force output in the injured muscle, supporting that overly inhibiting fibrosis may be detrimental retained [106]. These findings suggesting that a functional fibrosis forms across the injury defect, allowing some aspects of force transmission to be retained. While fibrosis may act to preserve some function following VML injury, the ultimate goal of regenerative medicine is to repair the lost muscle with new, healthy muscle. True regeneration cannot occur without mediating the inflammatory response and reducing the extensive fibrotic development.

While the most recognizable consequences of VML injury is a reduction in contractile function, robust inflammation, and fibrotic development, there are farther reaching consequences to organism health, including dysregulated skeletal muscle oxidative metabolism. Such impairments are readily observed by assessing the quality of oxidative muscle (e.g., type I fibers) and mitochondria. In a porcine study by Chao et al., VML injury resulted in an increase in the proportion of type I muscle fibers and increased mitochondrial number, however, type I fibers had reduced cross sectional area in VML-injured animals compared to controls and increased mitochondrial fission [107]. In a murine study by Aurora et al., the master regulator of mitochondria, PGC-1α, as expected was upregulated in response to rehabilitation in uninjured, but unexpectedly not in VML-injured animals [108]. Recently, Southern et al. found that the mitochondrial network is dysregulated after VML in a murine model [98]. Notably, Southern and colleagues found that overexpression of PGC-1α by means of transfection was able to rescue mitochondrial function as well as 32% of specific muscle torque, however when

compared to controls, a torque deficit of ~45% remained. These findings support initial evidence that oxidative metabolism is impaired following VML injury, and that mitochondrial functions may provide insight into potential routes of treatment, however, there is a lack research on how whole-body metabolism is affected by VML injury.

The major gaps in the current understanding go beyond muscle-specific metabolism and relate to how whole-body metabolism is affected by VML. This understanding is multifold. While poor metabolic outcomes are hypothesized following orthopaedic trauma, it is unknown how whole-body metabolism is affected following VML injury. No study to date has characterized whole-body metabolism in any organism following VML injury. Additionally, literature is lacking evaluation of physical activity levels following VML injury, either initially or well into the recovery period. Patients are expected to undergo bedrest and sedentarism following the initial VML injury, but it is unknown if animal models of VML exhibit similar patterns. Further, while it is clear that skeletal muscle function is severely impaired following VML injury, it is unclear how physical activity and metabolic function is linked to muscle contractile and oxidative activity, capillarity, and muscle fiber type distribution. To address the important questions raised above, my thesis had the following specific aims and hypotheses:

Specific Aim 1: Characterize physical activity and metabolism in mice chronically following VML injury.

Hypothesis 1: Physical activity will be reduced both acutely and chronically as a result of VML. This impairment is expected to contribute to a reduction in metabolic rate and respiratory exchange ratio (RER).

Specific Aim 2: Determine how VML injury impairs contractile and oxidative profile by assessing force output, muscle fiber cross sectional area, mitochondrial enzyme activity, and capillarity.

Hypothesis 2: Skeletal muscle will present functional and metabolic impairments in response to VML injury, including reduced force generating capacity, lower fiber cross-sectional area, reduced mitochondrial enzyme function, and lower capillarity.

These specific aims and hypotheses are addressed in Chapter 2, which include the final manuscript of my research project (in preparation for submission to *BMC Musculoskeletal Disorders*). Finally, Chapter 3 outlines future directions for this work.

Chapter 2: Research Project

Overview

Background: Volumetric muscle loss (VML) injuries result in a non-recoverable loss of muscle tissue and function due to trauma or surgery. Broadly, reductions in physical activity, as observed following orthopedic injury, increases the risk of metabolic inflexibility, a state where inefficiencies in fuel utilization may result in disease and comorbidity. It is likely that whole-body physical activity and metabolism are reduced post-VML injury, however these aspects remain uncharacterized. Our goal was to characterize whole-body physical activity and metabolism following VML injury, and to further investigate possible muscle fiber specific changes. **Methods:** Adult male C57Bl/6J (n=28) mice underwent a standardized VML injury to the posterior compartment of the hind limb (or control). Mice underwent longitudinal evaluation of whole-body physical activity and metabolism in specialized cages up to three times over the course of 8-weeks. At terminal time points of 4- and 8-week post-VML in vivo muscle function of the posterior compartment was elevated. Additionally, gastrocnemius muscle was collected to understand histologically and biochemically changed in the muscle remaining after VML. **Results:** The VML injury to the hind limb resulted in changes to the muscle and whole-body metabolism, despite no changes in physical activity. Reductions in whole-body metabolism occurred, largely driven by lower carbohydrate utilization during active hours. Contractile function of the injured limb was impaired due to a loss of fast muscle fibers, while slow muscle fibers were maintained. Though slower, oxidative muscle proportion increased, capillarity and biochemical activity of the muscle were not improved. Though there was an acute increase in activity of complex I of the electron transport chain, a lack of increase in up or downstream mitochondrial enzymes supports that mitochondrial uncoupling may occur following VML, which may contribute to impaired glucose metabolism and an increased risk of metabolic comorbidity. **Conclusions:** These findings support that alterations in VML-injured muscle may lead to impairments in whole-body metabolism. Future therapeutic efforts may be needed to improve health and function following VML.

Background

As the primary organ of movement and thermogenesis [1], skeletal muscle must utilize fuel from energy yielding sources, primarily carbohydrates for high workloads [109] and lipids for low workloads and rest [110]. Transitions between fuel sources occur due to various demands on the body and is represented by the degree of metabolic flexibility. Metabolically healthy individuals are able to efficiently transition between fuel sources with changing energetic demand, such as when transitioning between activity and rest, as well as times of fasting and feeding [88]. Energetic demands during exercise are an excellent example of robust metabolic flexibility as the body can physiologically match fuel availability with energy demands. In contrast, as individuals become metabolically unhealthy, such as in pathologic conditions of type II diabetes and obesity, they tend to become metabolically inflexible, or inefficiently able to transition between fuel sources [111]. Inactivity and lack of exercise are linked to greater all-cause mortality and have been shown to cause atherosclerosis, reduced cardiac function, type II diabetes, and obesity [87]. Further, physical inactivity has been implicated as a factor driving the onset of metabolic inflexibility [112,113]. Given that skeletal muscle is the primary organ of movement and lack of movement is linked to metabolic inflexibility, conditions that impair the ability of muscle to do physical work, such as orthopaedic traumas, may increase the risk of metabolic impairment in affected individuals both acutely and chronically.

Large-scale orthopaedic traumas have broad implications on long-term health and function and can potentially increase risk for metabolic comorbidities. For example, in patients who sustained fracture to the upper or lower extremities there are known decreases in physical activity and increases in sedentarism acutely following injury [85,86]. Similarly, various orthopaedic injuries and traumas result in decreases in physical activity as early as three months after initial injury [114]. One injury of particular significance is volumetric muscle loss (VML) injury, in which a substantial piece of a muscle or muscle unit is abruptly removed, resulting in chronic loss of muscle function and range of motion [115]. Currently, the long-term

comorbidities secondary to VML injury are not well understood, however, it is expected that there is a loss of skeletal muscle metabolic and physical activity. It is anticipated that after initial VML injury there will be periods of reduced mobilization that are unavoidable during prolonged care. It is thus hypothesized that patients with VML injury could be more likely to undergo periods of reduced physical activity and subsequently develop metabolic inflexibility chronically.

We posit that the sequela of VML injury includes impaired whole-body metabolism due to low physical activity and the loss of skeletal muscle tissue. Previous work in animal models of VML has indicated that skeletal muscle specific oxidative function is impaired following injury [98,107], and that the muscle remaining after VML injury has reduced metabolic plasticity compared to healthy, uninjured muscle in response to rehabilitation [116]. Dysfunction of skeletal muscle metabolism may impede the endogenous healing process and induce further chronic dysfunction. To date it is unknown to what extent VML injury impacts whole-body metabolism and physical activity both in animal models of VML injury or the patient population. The studies herein were designed to first understand if VML injury results in reduced physical activity and whole-body metabolism corresponding to chronic metabolic inflexibility. Second, to evaluate contractile and oxidative physiology of the skeletal muscle fibers after VML injury.

Methods

Animals and Study Design

Adult male C57Bl/6J (n=28) mice were purchased from Jackson Laboratories (Stock # 000664; Bar Harber, ME). Mice were allowed at least one week of acclimation to the facility prior to initiating any aspect of the study protocol. All protocols and animal care guidelines were approved by the University of Minnesota Institutional Animal Care and Use Committee (Protocol 1803-35671A), in compliance with the National Institute of Health Guidelines and the United States Department of Agriculture. All studies were conducted in compliance with the Animal Welfare Act, the Implementing Animal Welfare Regulations and in

accordance with the principles of the Guide for the Care and Use of Laboratory Animals.

Mice were housed on a 12-hour light-dark cycle (light phase begins at 06:00) with *ad libitum* access to standard chow and water. At ~12.5 weeks of age mice were allocated by rank order scheme assignment of respiratory exchange ratio, into VML injury (n=12), sham surgery (n=12), or injury naïve controls (n=4). Mice in the sham and naïve groups were not different and combined into a control group. Physical activity and metabolic assessments were conducted using Comprehensive Lab Animal Monitoring System (CLAMS; Columbus Instruments) at approximately 1-week pre-surgery and 2- and 6-weeks post-surgery for all animals. *In vivo* muscle function was assessed terminally 4- and 8-weeks post-surgery. Immediately following muscle function assessments, mice were euthanized with pentobarbital (>100mg/kg; s.q.), and skeletal muscles were harvested and frozen at -80^{o}C for later analyses.

Physical Activity and Metabolic Assessment

Mice were acclimated to individual CLAMS cages for 24-hours prior to each data collection period. The CLAMS system is a closed chamber that measures ventilation gases O_2 and CO_2 normalized to body mass (ml/kg/hr) to quantify metabolic activity. The respiratory exchange ratio (RER) is calculated as the volume ratio of CO_2 and O_2. Calorific value (CV) is the relationship between heat and oxygen consumption, as described in Graham Lusk's "*The Elements of the Science of Nutrition*" [117] by the following equation: CV = 3.815 + 1.232 * RER. Further, energy expenditure (i.e., heat) is calculated as the product of the CV and the VO_2 of the mouse and represents the metabolic rate.

Each CLAMS cage is equipped with infrared beams in the X, Y, and Z axes that register physical movement when the beam array is broken. Individual beam breaks are classified as activity counts. When the mouse is moving in the same position (i.e., grooming, drinking, and feeding), the movement is tracked as a count. As multiple beams in sequence are broken, the movement is tracked as

ambulatory counts. Beams along the X and Y axis are spaced at 1.27cm intervals, allowing quantification of ambulatory distance.

Data were collected and analyzed using CLAMS data examination Tool (Clax, v2.2.15; Columbus Instruments), a software integrated with CLAMS for the 24-hour periods. Data for total counts and ambulatory counts were collected in 10-second increments, and RER, metabolic rate, VO_2 and VCO_2 were collected in 4-minute increments. All data were subsequently exported for later analyses.

Overall data were analyzed in bins of 24, 12 (active vs. inactive time periods), 6, and 1 hour and presented as a mean over the time period. Metabolic flexibility was measured by assessing the range of metabolic rate and RER as the delta between 12-hour active and inactive values. Each incremental RER and metabolic rate data were also used to calculate hourly moving averages using an average of every 15, 4-minute increment. The moving averages were used to evaluate the area under the curve (AUC) as a more specific measure of metabolic flexibility.

Volumetric Muscle Loss (VML) Surgical Procedure

As previously described [98,116], the VML injury was a full thickness injury to the posterior compartment muscle group (gastrocnemius, soleus, and plantaris muscles). A subset of mice underwent sham VML procedures or no surgical procedure (injury naïve). About 2 hours prior to surgery mice received SR buprenorphine (1.2mg/kg; s.q.) for pain management. Mice were anesthetized using isoflurane (1.0-3.0%) under aseptic surgical conditions. A posterior-lateral incision was made through the skin to reveal the gastrocnemius muscle. Blunt dissection was used to isolate the posterior muscle compartment, and a metal plate was inserted between the tibia and the deep aspect of the soleus. A 4 mm punch biopsy (20.9±4.9 mg, ~15% volume loss of muscle) was performed on the middle third of the muscle compartment. Any bleeding was stopped with pressure. Incisions were closed with 6.0 silk sutures and animals were monitored through recovery.

In vivo muscle function

At the terminal time point (4- or 8-weeks post-injury) the isometric torque of the posterior compartment muscle was evaluated as previously described [98,116]. Briefly, *in vivo* isometric torque was measured in anesthetized mice (isoflurane 1.5–2.0%) while body temperature was maintained at 37^{o}C. The foot was positioned to a footplate attached to a dual-mode muscle lever system (Model 129 300C-LR; Aurora Scientific, Aurora, Ontario, Canada). The knee was secured using a custom-made mounting system, and the ankle was positioned at a 90^{o} angle. First, under computer control of the servomotor, the ankle was passively rotated 20^{o} from neutral in both the plantar- and dorsi-flexion directions (total 40^{o} of motion). Second, to avoid recruitment of the anterior compartment muscles, the common perineal nerve was severed. Platinum-Iridium percutaneous needle electrodes were placed across the sciatic nerve, which branches to the tibial nerve. Then optimal muscle stimulation was achieved by finding peak-isometric torque by increasing the current in increments of 0.2 mAmps. The force frequency relationship was assessed by measuring torque as a function of the following stimulation frequencies: 5, 10, 20, 40, 60, 80, 100, 150, and 200 Hz. Isometric torque is expressed as mN·m to determine absolute functional capacity or per kg body weight to assess functional quality.

Biochemical Analysis

At the terminal time points, the proximal and distal thirds of the gastrocnemius muscle of all animals were snap frozen using liquid nitrogen and subsequently stored at -80°C until biochemical analysis. The distal third portion was weighed and homogenized in 10mM phosphate buffer (pH 7.4) at a ratio of 1:10 (mg/µl), using a glass pestle tissue grinder. Total protein content was analyzed in triplicate and averaged using the Protein A280 setting on a NanoDrop One spectrophotometer (Thermo Scientific). Mitochondrial content was analyzed by citrate synthase enzyme activity as previously described [98]. The proximal third portion of the gastrocnemius muscle remaining was homogenized in 33mM

phosphate buffer (pH 7.4) at a muscle to buffer ratio of 1:40 using a glass tissue grinder. Homogenate was incubated with 5,5'-dithio-bis (2-nitrobenzoic acid (DTNB, 0.773 mM), acetyl CoA (0.116 mM), and oxaloacetate (0.441 mM) in 100 mM Tris buffer (pH 8.0). Activity of citrate synthase activity was monitored from the reduction of DTNB over time via measurement of absorbance at 412 nm.

Histological and Morphologic Analyses of Muscle Fibers

At harvest, the middle third of the gastrocnemius muscle of all animals was isolated for histological evaluation. Muscles were mounted on cork using tragacanth gum, frozen in 2-methylbutane cooled by liquid nitrogen, and subsequently stored at -80°C. Ten µm sections of the mid-belly of the gastrocnemius muscle were collected using a Leica cryostat and microtome. Serial sections were stained first with Masson's Trichrome for qualitative analysis of skeletal muscle fibers and fibrotic deposition and quantification of centrally-located nuclei. Subsequently, sections were stained to quantify capillarity, nicotinamide adenine dinucleotide hydrogen (NADH)- tetrazolium reductase and succinate dehydrogenase (SDH) to identify and quantify the proportion of oxidative muscle fibers, and myosin heavy chain (MyHC) fiber type composition.

Capillarity was assessed by staining for alkaline phosphatase activity [118]. Muscles were incubated in alkaline phosphate buffer for one hour at 37°C. Sections were then washed, incubated with 0.25% metanil yellow for five minutes, and washed again. NADH-TR staining was performed by incubating tissues at 37°C for 20 minutes in a solution containing 0.2M Tris, 1.5 mM NADH, and 1.5 mM NBT [119]. Sections were washed, dehydrated, and cleared in xylenes. SDH staining was performed by incubating tissues at 37°C for one hour in a 0.2M sodium phosphate buffer solution [120]. Tissues were rinsed, dehydrated in graded acetone dilutions, and rinsed again.

Frozen muscles were also analyzed for MyHC isoform expression. Staining of the gastrocnemius muscle was completed with a combination of primary antibodies, including anti-$MyHC_{slow}$ (BA-D5, 5µg/ml), anti-$MyHC_{2A}$ (SC-71,

5µg/ml), and anti-$MyHC_{2B}$ (BF-F3, 5µg/ml) all acquired from the Developmental Hybridoma Studies Bank (Iowa City, IA). Additionally, sections were stained with wheat germ agglutinin (Invitrogen W7024, 1 µg/ml) to identify the sarcolemma. Appropriately paired secondary Alexa-Fluor (Invitrogen A21240) and DyLight (Jackson ImmunoResearch 115-475-207 or 115-545-020) conjugated antibodies at a dilution of 1:200 were used. In all cases, the expected staining patterns in normal skeletal muscle were observed and the specificity of anti-labeling was confirmed by the absence of staining outside expected structures and was consistent with manufacturer's technical information. The specificity of the MyHC isoform antibodies has been previously validated [121] and is representative of our previous work [122,123].

All brightfield images were acquired using the TissueScope LE slide scanner (Huron Digital Pathology, St. Jacobs, ON, Canada) using a 20X objective (0.75 NA, 0.5 µm/pixel resolution). Following imaging, using HuronViewer (Huron Digital Pathology), three standardized regions of interest (ROI) were selected for each muscle and exported for analysis. All ROIs were standardized to 500 x 500µm. One ROI was created to encompass the area immediately adjacent to the defect region of the VML group and two ROIs encompassed the remaining skeletal muscle tissue on medial and lateral side of the defect region. The corresponding three ROI areas were also obtained in muscles of the control groups. All ROIs were systematically used across all muscles from the same animal. The ROIs were first evaluated independently within the respective region (lateral, mid-muscle, and medial). Subsequently, data from these ROIs were either summed or averaged across the gastrocnemius muscle and compared across groups.

Fluorescent images of all muscles stained for MyHC isoform expression was conducted using a Nikon C2 automated upright laser scanning confocal microscope equipped with a Plan Apo λ 20x objective and dual GaSP detectors (Nikon Instruments Inc., Melville, NY). Image sampling was determined using Nyquist calculations with a pixel size set to 0.31µm and pixel dimension of 2048 x

2048. Images were collected from the same three ROIs previously described. All ROIs were subsequently saved and exported for analysis.

Analyses of muscle sections were conducted using Fiji [124]. The multipoint tool was used to manually count muscle fibers, centrally located nuclei, and capillaries, as well as the number of darkly and lightly stained muscle fibers for all NADH and SDH stained muscle. Darkly stained fibers were classified as positive for NADH and SDH, indicating high metabolic activity, while lightly stained fibers were classified as negative for NADH and SDH, suggesting low metabolic activity. Fibers of the gastrocnemius muscle were classified signally as type I, IIa, and IIb based on the expression of $MyHC_{slow}$, $MyHC_{2A}$, and $MyHC_{2B}$, respectively. Fibers were classified as type IIx based on the absence of staining. Additionally, muscle fiber cross-sectional area (CSA) was measured for each section using the freehand tool and quantified as fiber-type specific CSA. Muscle CSA was only quantified for fibers between 50-7,500μm^2. For display purposes only, images were down-converted, without introducing any changes in brightness or contrast and produced in Adobe Photoshop (Adobe Systems Inc.). During all imaging laser intensity was kept consistent across imaging of the same probes. Investigators were blinded during all imaging and post-imaging analyses.

Statistical Analyses

Data analysis was conducted using JMP (version 14.3.0, SAS Institute, Inc.) and Prism (version 9, GraphPad Inc). For metabolic and physical activity data, one-way ANOVAs were used to evaluate differences across time frames of 1-, 6-, 12-, and 24-hr periods. Longitudinal differences across time, pre-VML and 2- and 6-weeks post-VML were calculated using means and AUC, differences were evaluated using one-way, repeated measures, ANOVA. One-way ANOVAs were used to evaluate differences across groups for body weight, muscle weight, muscle function, histologic parameters, and protein and enzyme content. Two-way ANOVAs were used to evaluate overall muscle fiber-type specifics differences across group. Distributions of capillaries per muscle fiber and fiber CSA were

evaluated by chi-squared, and alpha was corrected for multiple comparisons at 0.167. When appropriate Tukey's HSD post hoc was evaluated, significance was set at an alpha of 0.05. Data is reported as mean ± SD unless noted otherwise.

Results

Animals

During the pre-VML metabolic and physical activity evaluation, mice weighed 27.7±2.0g on average. As expected, mice gained weight over the 4- and 8-week period, with an average terminal body mass of ~30 and 31g, respectively (**Table 2**). Body weight was not significantly different between experimental groups at any time during the study duration (p=0.123). Following all surgical procedures mice recovered promptly and no adverse events were identified.

Table 2. Contractile properties following VML injury

	Control	VML 4-week	VML 8-week	p-value
	(n=16)	(n=5)	(n=7)	
Body weight (g)	30.5 ± 0.6	29.3 ± 1.1	31.1 ± 0.9	0.427
Gastrocnemius weight ratio	1.08 ± 0.08	0.84 ± 0.07 *	0.92 ± 0.15 *	<0.001
Passive torque (mN·m)	2.4 ± 0.5	4.2 ± 1.4 *	5.1 ± 1.4 *	<0.0001
Peak twitch 5Hz (mN·m)	4.1 ± 0.9	2.9 ± 0.7 *	1.9 ± 1.0 *	<0.0001
Peak torque (mN·m)	19.2 ± 2.5	12.3 ± 1.2 *	9.9 ±2.4 *	<0.0001
Twitch:tetani ratio	0.21 ± 0.01	0.23 ± 0.02	0.19 ± 0.02	0.313

Data analyzed by one-way ANOVA, presented as mean ± SD. Different than *control

Baseline physical and metabolic activity

Prior to allocation into experimental groups, all mice were analyzed for 24-hour physical and metabolic activity. At this baseline time point, mice ambulated 1.3±0.3km over 24 hours, with ~1km ambulated during the active period (i.e., dark hours of 18:00-06:00) and the remaining over the inactive period (i.e., light hours of 06:00-18:00). Over the course of 24 hours, the average metabolic rate was ~19 kcal/hr, with an expected greater metabolic rate during the active period (~21 kcal/hr) and lesser during the inactive period (~17 kcal/hr, p<0.001; **Figure 1A**). Metabolic flexibility, as quantified by the delta metabolic rate, was approximately 4.5kcal/hr. Metabolic rates fluctuated between 19-24 kcals/hr during the active period and were greatest early in the active period, specifically from 18:00-22:00

(p<0.001; **Figure 1C**). During the inactive period, metabolic values fluctuated between 15-19 kcal/hr with the greatest values occurring during the transition from active to inactive, around 05:00-08:00 hours. Hourly metabolic rate was typically below 17 kcals/hr during the rest of the inactive time period (p<0.001).

The RER over the course of 24 hours was ~0.90, with a RER of ~0.93 during

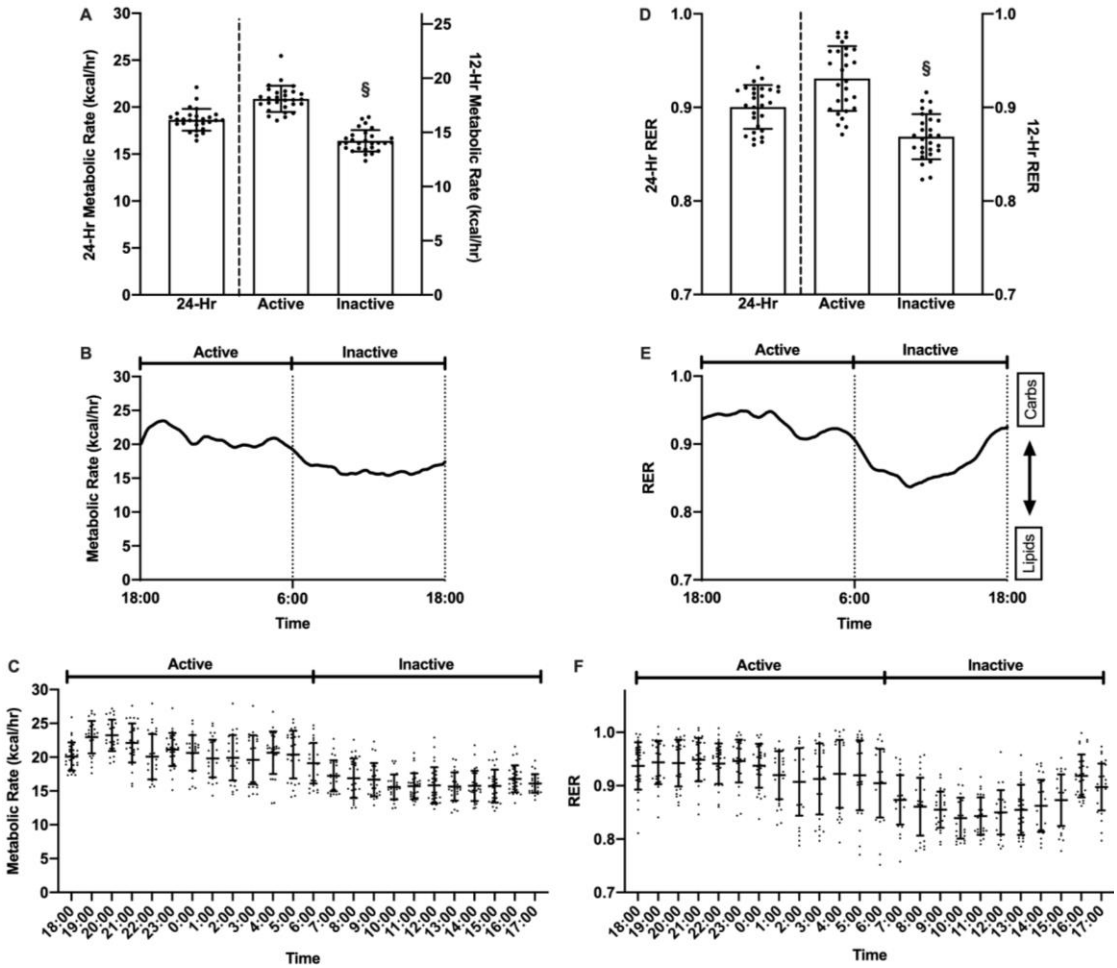

Figure 1: Mice were evaluated for whole-body metabolism and physical activity ~1-week prior to allocation into experimental groups, data was collected over 24 hours in a specialized closed cage system; while mice were housed in a 12-hour light: dark environment matching the inactive and active time periods, respectively. Both metabolic rate and respiratory exchange ratio (RER) were analyzed in 1-, 12-, and 24-hour bins. **A)** Metabolic rate was highest during the 12-hour active period, which was significantly greater than during the 12-hour inactive period (p<0.001). **B)** The total area under the curve (AUC) for metabolic rate was 5936±33. **C)** In 1-hr bins the greatest metabolic rate recorded during the active period. **D)** Similarly, the greatest RER occurred over the 12-hour active period, which was significantly greater than RER during the inactive period (p<0.001). **E)** The RER followed the same trend as the metabolic rate, with an AUC of 63.8±0.61, and **F)** the greatest RER values occurred during the active period, suggestive of greater carbohydrate utilization during this phase. Data presented as mean±SD; analyzed by one-way ANOVA; significantly different from §active period.

the active period but only ~0.87 during the inactive period (p<0.001; **Figure 1D**), suggesting a greater carbohydrate utilization during the active period, and greater lipid utilization during the inactive period. Hourly RER fluctuated between 0.90-0.96 during the active period, with a gradual decline during the transition to the inactive period from 05:00-11:00. Inactive RER values fluctuated between 0.84-0.93, with the lowest values occurring during the middle of the active period from 11:00-13:00, then gradually increasing from through 17:00 (p<0.001; **Figure 1F**).

VML-induced changes in physical and metabolic activity

Following VML injury both physical and metabolic activity were longitudinally evaluated in a subset of mice at pre-, 2- and 6-weeks post-VML surgery. There was no difference in physical activity, specifically ambulatory distances, longitudinally after VML injury. The total distances ambulated for pre-, 2- and 6-weeks post-VML were 1.3±0.3, 1.4±0.2, and 1.4±0.4km, respectively (p=0.809). As expected, most of the ambulatory activity occurred during the active time period.

Longitudinal metabolic activity measurements supported a decrease in metabolic rate by 6-weeks post-VML, specifically the 24-hour metabolic rate decreased ~10% compared to pre- and 2-weeks post-VML (p=0.012; **Figure 2A**). Similarly, metabolic rate was decreased ~9% by 6-weeks post-VML during the active period compared to 2-weeks post-VML (p=0.032) and was reduced ~12% by 6-weeks compared to pre- and 2-weeks post-VML, during the inactive period (p=0.092; **Figure 2A**). There was no difference in delta metabolic rate at any time point evaluated (p=0.988; **Figure 2B**). To specifically evaluate possible differences in metabolic flexibility, metabolic rate was also compared across time points with the calculated AUC. The 24-hour metabolic rate AUC was significantly decreased by 6-weeks post-VML (5,400±30) compared to pre- and 2-weeks post-VML (5948±33 and 6026±30, p<0.001; **Figure 2C**). Subsequently, the AUC was evaluated in 6-hour bins. Within each active 6-hour bin, the metabolic rate 6-weeks post-VML was significantly reduced compared to the pre-VML and 2-weeks post-

VML time points (p≤0.001; **Figure 2C**). Only during the second phase of the inactive period (00:00–06:00) was the metabolic rate at 2-weeks post-VML different from pre-VML (p=0.007; **Figure 2C**).

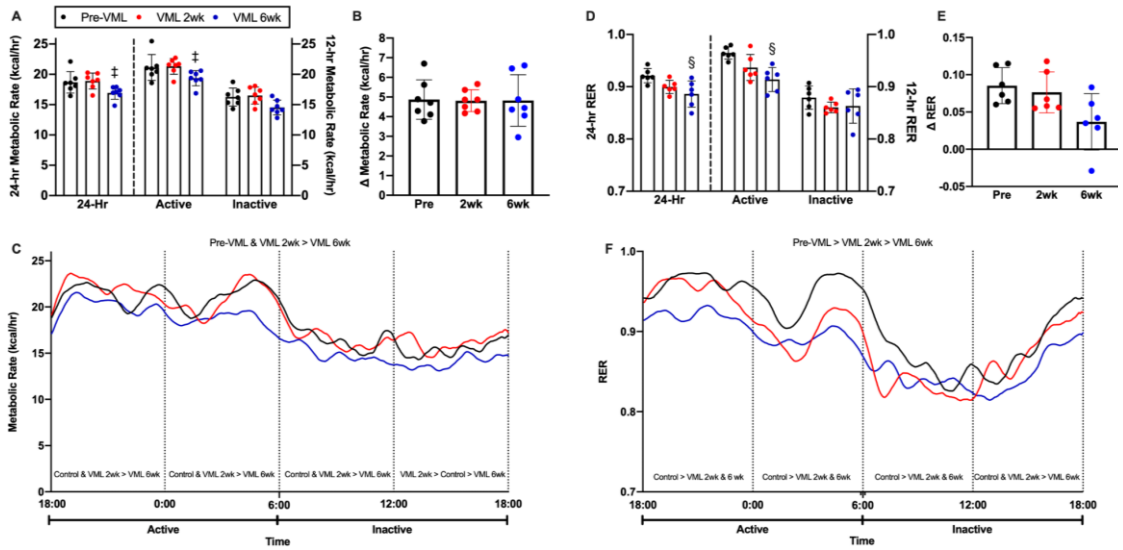

Figure 2: In a subset of mice, longitudinal evaluation of metabolic rate and RER was conducted pre-VML surgery and at 2- and 6-weeks post-VML surgery. **A)** By 6-weeks post-VML, mice had an ~10% decreased metabolic rate during the 24-hour and 12-hour active periods, compared to 2-weeks post-VML (p≤0.050). **B)** No differences were observed across time for the delta in metabolic rate between the active and inactive periods (p=0.988). **C)** Metabolic rate was evaluated by comparing the AUC values across time. When broken into 6-hour bins, significant differences are noted across time points within each bin, with mice at 6-weeks post-VML demonstrating the lowest metabolic rate in each 6-hour bin (p≤0.007). **D)** The RER at 6-weeks post-VML was decreased ~4% over 24 hours compared to the pre-VML, indicating reduced carbohydrate oxidation and daily caloric expenditure (p=0.013). This decrease was likely due in part to a significant reduction in RER which occurred during the active period by 6-weeks post-VML (p=0.002). **E)** There were no differences across time were determined for the delta RER (p=0.530). **F)** At 2-weeks post-VML, mice exhibited a lower RER as determined by AUC compared to pre-VML, and a further significant reduction in RER at 6-weeks post-VML, indicating progressively impaired metabolic flexibility 2- and 6-weeks post-VML compared to baseline (p<0.001). When analyzed in 6-hour bins, significant differences were observed across evaluation time points for each bin (p≤0.001). Data presented as mean±SD; analyzed by one- or two-way ANOVA; significantly different from §pre-VML; ‡VML 2wk.

In addition to metabolic rate, RER was evaluated longitudinally. At 6-weeks post-VML 24-hour RER was significantly reduced by ~4% compared to the pre-VML (p=0.014), likely due to the reduction in RER during the active time (p=0.003; **Figure 2D**). There was no difference in the delta RER over time (p=0.530; **Figure 2E**). The 24-hour metabolic flexibility in RER was significantly lower at 2- and 6-weeks post-VML compared to pre-VML (AUC 279±1, 284±1 vs. 291±1, p<0.001; **Figure 2F**). The RER during the active period was greatest pre-VML, and lowest

at 6-weeks post-VML, particularly during the first 6 hours of the active period ($p<0.001$; **Figure 2F**). A similar pattern was observed during the inactive period, in which the RER pre-VML was the greatest, while at 6-weeks post-VML RER was the lowest, especially during the second phase of the inactive period ($p<0.001$; **Figure 2F**). Collectively, indicating an impairment in metabolic flexibility up to 6-weeks following VML injury.

In vivo muscle function

The VML injury to the posterior compartment resulted in an ~22% reduction of gastrocnemius mass at 4-weeks, and ~15% reduction at 8-weeks ($p<0.001$; **Table 2**). The passive torque at 20º of dorsiflexion was determined as a surrogate of passive muscle stiffness. The VML injury resulted in a significant increase in passive torque about the ankle joint by ~2 fold at 4-weeks and 8-weeks ($p<0.001$; **Table 2 & Figure 3**). The VML injury did not impact the twitch to tetani ratio of the ankle plantar flexor muscles (**Table 2**).

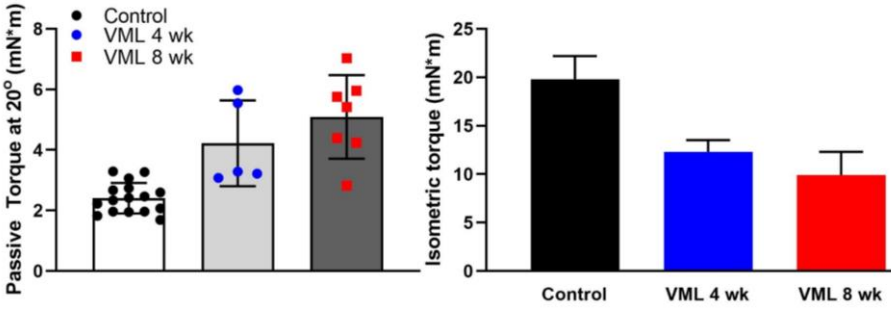

Figure 3: *In vivo* muscle function was normalized for body weight. **A)** The passive torque of the ankle plantar flexor muscles at 20° dorsiflexion was greatest at both 4- and 8-weeks following VML ($p<0.001$). **B)** The peak isometric torque of the ankle plantar flexor muscles was significantly reduced at both 4- and 8-weeks following VML ($p<0.001$). Data presented as mean±SD; analyzed by one-way ANOVA; significantly different from *control.

There was no difference in the force-frequency (1-300 Hz) relationship of the ankle plantar flexor muscles, maximal torque was reached at a frequency of 200 Hz, and the ~50% torque deficit in the VML group was observed at various frequencies from 40-80 Hz. Compared to controls, maximal isometric torque of the ankle plantar flexor muscles decreased by about 50% at both 4-weeks and 8-weeks

post-VML ($p<0.001$; **Table 2 & Figure 3**). Both absolute and torque normalized to body mass were significantly impaired by VML injury.

Biochemical analysis of gastrocnemius muscles

The remaining gastrocnemius muscle had minimal VML-induced changes to total protein content ($p=0.674$). Similarly, citrate synthase activity, a surrogate of mitochondrial abundance, was also unchanged ($p=0.444$). There were also no differences in succinate dehydrogenase activity ($p=0.128$). Collectively, biochemical aspects of the gastrocnemius appear largely unchanged post-VML (**Table 3**).

Table 3. Biochemical composition of gastrocnemius muscle following VML

	Control	**VML 4-week**	**VML 8-week**	**p-value**
	(n=16)	(n=5)	(n=7)	
Total protein content (mg/mg muscle)	20.4 ± 3.4	19.3 ± 3.6	18.7 ± 2.4	0.674
Citrate synthase (µmol/min/g)	498.8 ± 75.4	458.0 ± 77.8	480.3 ± 116.3	0.444
Succinate dehydrogenase activity (µmol cyto c/min/g)	4.93 ± 0.68	4.12 ± 0.95	4.86 ± 0.80	0.128
Data analyzed by one-way ANOVA, presented as mean ± SD				

Histological analysis of gastrocnemius muscles

Whole muscle and regional histologic characteristics of gastrocnemius muscles were evaluated terminally across experimental groups. In comparison to control muscles, qualitative examination showed fibrotic development in muscles post-VML with some muscle fibers that appeared smaller in size and irregular in shape and there was an abundance of centrally-located nuclei, particularly in the medial portion of the muscle near the initially created VML injury (**Figure 4**).

Specific changes in the VML-injured gastrocnemius muscle fibers were quantified across the muscle (**Table 4**). The lateral and medial regions did not experience a change in capillaries per fiber ($p\geq0.345$), while the mid-region bordering the VML defect demonstrated a reduction in capillaries at 4-weeks and an increase at 8-weeks post-VML ($p=0.041$). Across the entire gastrocnemius muscle, there was a difference in the distribution of capillaries per muscle fiber

muscle at both 4- and 8-weeks post-VML compared to control ($p<0.001$). Between the 4- and 8-weeks post-VML groups there was also a leftward shift in capillary distribution ($p=0.001$), in parallel with an increased proportion of capillaries per fiber at the tail ends of the distribution curve (**Figure 5A**). There were no differences between groups in the number of capillaries per muscle fiber across the whole gastrocnemius muscle ($p=0.154$; **Figure 5B**).

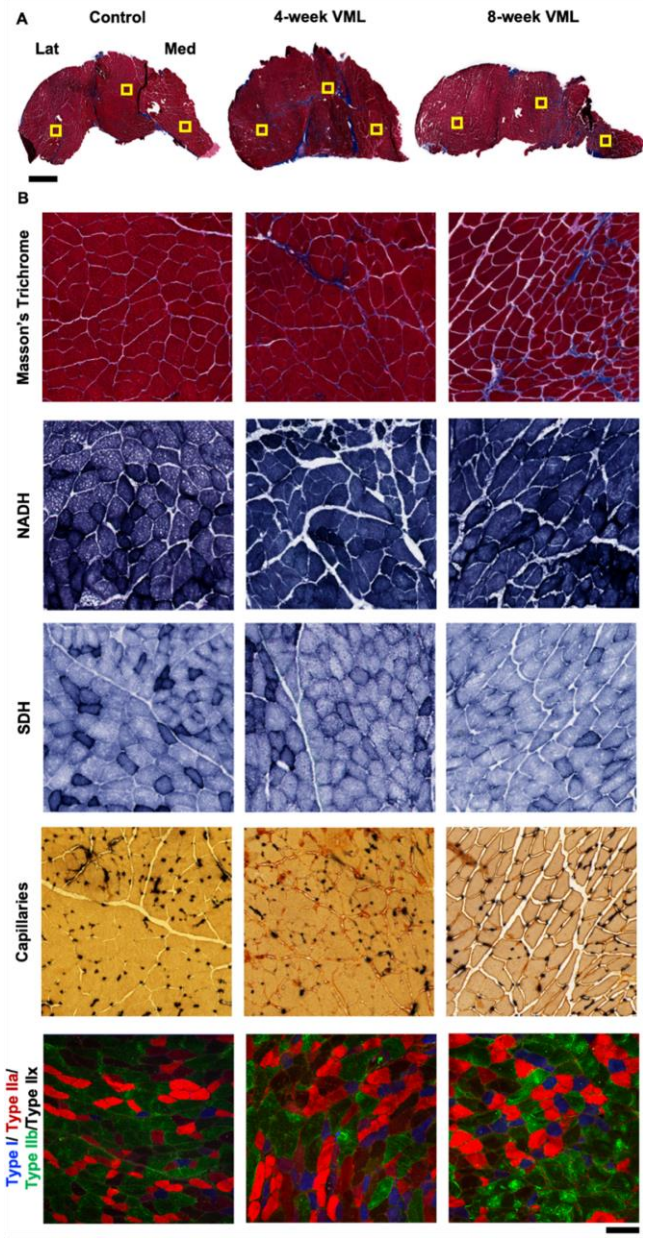

Figure 4: Histologic evaluation of the gastrocnemius muscle occurred at 4- and 8-weeks following VML injury and in control muscles. **A)** Representative whole gastrocnemius muscles for each group. Three standardized regions of interest were evaluated for each muscle (boxes), representing the lateral and medial aspects of the gastrocnemius muscle, as well as a mid-gastrocnemius region which is at the point adjacent to the VML injury. Scale bar is 1mm. **B)** Serial sections of the gastrocnemius muscle were stained for various physiologic and oxidative characteristics, and representative images from the medial/defect region are shown. Masson's Trichrome (staining muscle fibers red; fibrosis blue; nuclei black) was used to evaluate muscle quality and centrally located nuclei. NADH and SDH were used to evaluate oxidative enzymes, with darker stained fibers indicating fibers positive for NADH or SDH, respectively. Alkaline phosphatase was used to evaluate capillarity of fibers (staining muscle fibers yellow; capillaries black). Myosin heavy chain (MyHC) isoform expression was evaluated using antibodies for $MyHC_{slow}$, $MyHC_{2A}$, and $MyHC_{2B}$, or the absence of staining indicating types I, IIa, or IIb fibers, type IIx fibers in blue, red, green, or black, respectively. Scale bar is 100µm.

Table 4. Histologic composition of the muscle following VML				
	Control	**VML 4-week**	**VML 8-week**	**p-value**
Lateral Gastrocnemius				
NADH positive fibers (%)	75.1 ± 11.8	87.2 ± 2.7	85.0 ± 11.2	0.088
SDH positive fibers (%)	53.7 ± 20.2	72.5 ± 19.5	67.7 ± 16.8	0.163
Fibers with centrally located nuclei (%)	7.2 ± 8.2	20.2 ± 9.6	33.1 ± 31.6 *	0.013
Mean capillaries per fiber	5.6 ± 1.1	4.4 ± 1.0	4.8 ± 1.1	0.698
Mid-Gastrocnemius; VML border				
NADH positive fibers (%)	63.0 ± 18.0	78.7 ± 13.3	72.8 ± 15.9	0.202
SDH positive fibers (%)	30.6 ± 21.5	34.0 ± 23.6	25.8 ± 13.4	0.788
Fibers with centrally located nuclei (%)	1.6 ± 2.3	28.1 ± 14.1 *	18.7 ± 9.2 *	<0.001
Mean capillaries per fiber	3.6 ± 1.1	2.7 ± 1.0 *	3.9 ± 1.1 *	0.041
Medial Gastrocnemius				
NADH positive fibers (%)	71.5 ± 15.5	91.3 ± 1.5 *	59.6 ± 21.2	0.036
SDH positive fibers (%)	58.0 ± 13.8	66.4 ± 19.2	58.0 ± 16.0	0.663
Fibers with centrally located nuclei (%)	8.2 ± 12.8	21.8 ± 16.3 *	29.7 ± 13.9 *	0.005
Mean capillaries per fiber	4.6 ± 1.1	5.3 ± 0.6	5.2 ± 1.2	0.345
Data analyzed by one-way ANOVA, presented as mean ± SD. Different than * control				

The percentage of muscle fibers with centrally located nuclei was greater in the medial and mid-gastrocnemius regions at 4-weeks post-VML and in all regions at 8-weeks post-VML ($p \leq 0.013$; **Table 4**). At 8-weeks post-VML across the whole muscle, there was a greater percentage of central nuclei than controls ($p<0.001$) but a similar percentage to muscles at 4-weeks post-VML ($p=0.395$). There were no differences in the percentage of central nuclei between muscles of controls or at 4-weeks post-VML ($p=0.338$; **Figure 5C).** In examining the oxidative capacity of the muscle, expression of NADH-positive fibers was only different 4-weeks post-VML in the medial region compared to control ($p=0.036$), while no differences in SDH-positive fibers were observed in any region at any time point ($p \geq 0.163$; **Table 4**). Across the whole muscle, there was an increase in NADH-positive muscle fibers at 4-weeks post-VML compared to control but not compared to 8-weeks post-VML ($p \geq 0.022$). No differences in the percentage of NADH-positive fibers were observed between controls and 8-weeks post-VML (**Figure 5D**). There were no differences in percentage of SDH-positive muscle fibers across control, 4- or 8-weeks post-VML ($p \geq 0.278$; **Figure 5E**).

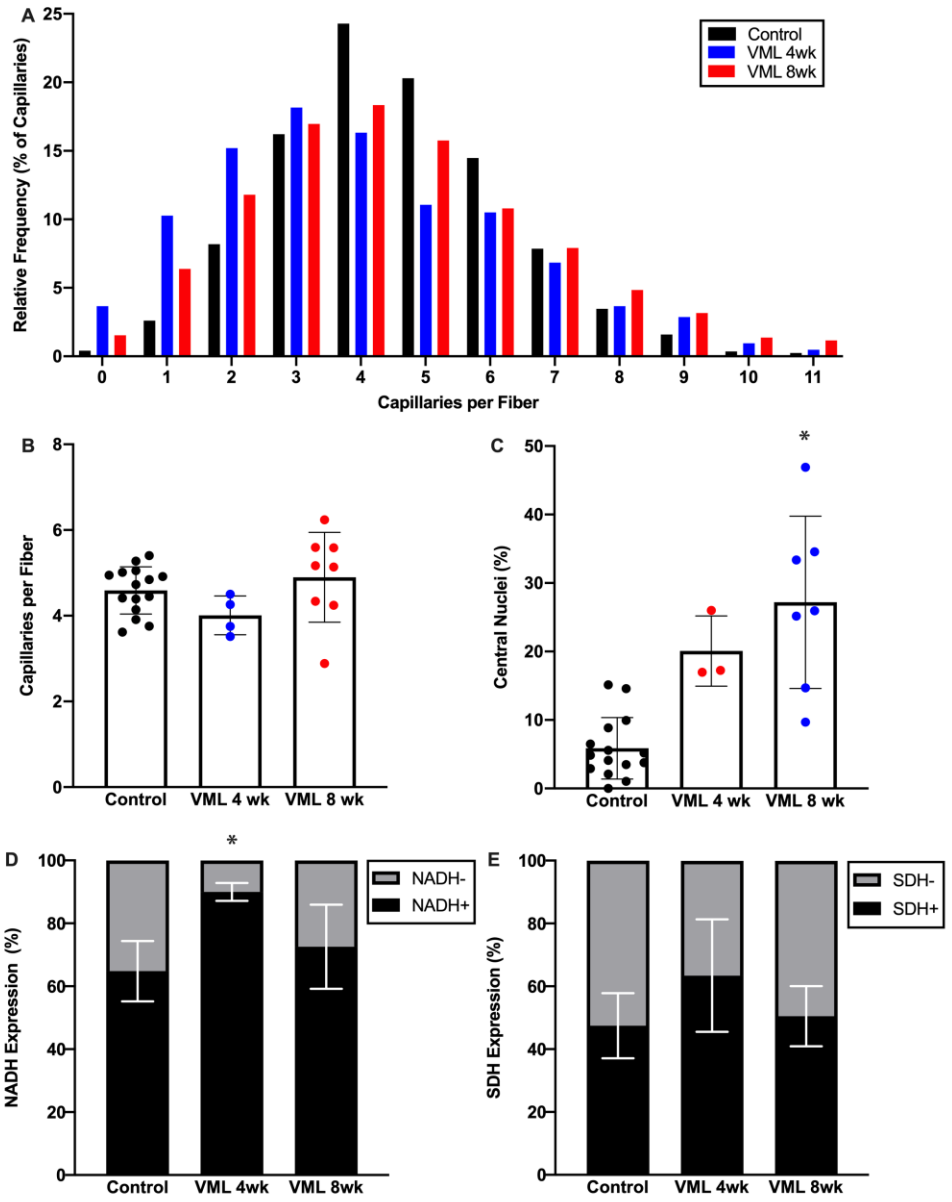

Figure 5: Capillarity and oxidative activity were evaluated in gastrocnemius muscle and compared across control, 4- and 8-weeks post-VML. **A)** The distribution of capillaries was significantly different at both 4- and 8-weeks post-VML compared to controls ($p<0.001$) and between groups at 4- and 8-weeks post-VML ($p<0.001$). **B)** There were no differences in the average number of capillaries per gastrocnemius muscle fiber ($p=0.154$). **C)** Compared to controls, muscles at 8-weeks post-VML had a greater percentage of centrally located nuclei ($p=0.007$), and this was similar to muscles at 4-weeks post-VML ($p=0.338$). **D)** There was a significant increase in NADH-positive fibers 4-weeks post-VML compared to controls ($p=0.016$) but not compared to 8-weeks post-VML ($p=0.059$). **E)** There were no significant differences were observed between control, 4- or 8-weeks post-VML ($p=0.625$). Data presented as mean±SD; analyzed by chi-squared and one-way ANOVA; significantly different from *control.

Gastrocnemius muscles were evaluated for fiber type specific differences in

fiber cross-sectional area following VML injury. Compared to control, the distribution of muscle fiber cross-sectional area shifted left at 4- and 8-weeks post VML ($p<0.001$), and VML groups were not significantly different than each other ($p<0.017$; **Figure 6A**). Within the gastrocnemius, fiber-type specific cross-sectional areas did not vary between groups at any time point ($p\geq0.070$; **Table 5**). However,

Table 5. Fiber type specific size of gastrocnemius muscle following VML

	Control	VML 4-week	VML 8-week	p-value
Lateral Gastrocnemius				
Type I (mean CSA μm^2)	1333.5 ± 249.4	1232.6 ± 431.9	1454.0 ± 334.6	0.917
Type IIa (mean CSA μm^2)	1416.9 ± 142.2	1278.0 ± 229.2	1530.7 ± 229.22	0.740
Type IIb (mean CSA μm^2)	3026.7 ± 239.8	2218.1 ± 428.95	2467.6 ± 391.6	0.205
Type IIx (mean CSA μm^2)	2211.7 ± 231.1	1906.3 ± 386.7	1771.9 ± 353.0	0.545
Mid-Gastrocnemius; VML border				
Type I (mean CSA μm^2)	1099.1 ± 163.4	680.6 ± 346.6	1009.5 ± 219.2	0.564
Type IIa (mean CSA μm^2)	1289.0 ± 148.7	1138.4 ± 284.7	1563.3 ± 186.4	0.383
Type IIb (mean CSA μm^2)	2977.7 ± 238.3	1792.7 ± 426.3	2595.0 ± 360.3	0.070
Type IIx (mean CSA μm^2)	1777.9 ± 179.7	1268.7 ± 311.3	1976.9 ± 235.3	0.213
Medial Gastrocnemius				
Type I (mean CSA μm^2)	834.7 ± 175.0	846.1 ± 234.7	1150 ± 234.7	0.535
Type IIa (mean CSA μm^2)	1241.6 ± 104.1	1104.1 ± 180.3	1165.6 ± 164.5	0.787
Type IIb (mean CSA μm^2)	2746.3 ± 219.5	2393.5 ± 392.6	2128.7 ± 331.8	0.296
Type IIx (mean CSA μm^2)	1597.4 ± 188.7	1641.4 ± 337.6	1791.3 ± 308.2	0.867
Data analyzed by one-way ANOVA, presented as mean ± SD. Different than *control				

a main effect of group was observed when analyzing cross-sectional area of type I, IIa, IIb, and IIx fibers across the whole muscle, where smaller cross-sectional areas were observed 4-weeks and 8-weeks post-VML compared to controls

Table 6. Fiber type specific composition of gastrocnemius muscle following VML

	Control	VML 4-week	VML 8-week	p-value
Lateral Gastrocnemius				
Percent of Type I Fibers	3.9 ± 1.9	9.1 ± 3.5	15.8 ± 3.2 *	0.012
Percent of Type IIa Fibers	20.4 ± 4.0	37.7 ± 7.1	32.6 ± 6.5	0.078
Percent of Type IIb Fibers	60.4 ± 6.5	35.8 ± 11.7	36.9 ± 10.6	0.083
Percent of Type IIx Fibers	15.2 ± 2.5	17.4 ± 4.4	14.7 ± 4.0	0.888
Mid-Gastrocnemius; VML border				
Percent of Type I Fibers	7.2 ± 3.5	15.7 ± 6.3	6.1 ± 5.3	0.451
Percent of Type IIa Fibers	19.2 ± 4.3	22.8 ± 7.7	26.5 ± 6.5	0.640
Percent of Type IIb Fibers	59.7 ± 7.6	54.7 ± 13.7	50.0 ± 11.5	0.777
Percent of Type IIx Fibers	13.9 ± 2.6	6.8 ± 4.7	17.4 ± 4.0	0.234
Medial Gastrocnemius				
Percent of Type I Fibers	3.9 ± 2.3	19.1 ± 4.1 *	13.4 ± 3.4	0.006
Percent of Type IIa Fibers	20.6 ± 3.4	39.5 ± 6.1 *	22.9 ± 5.2	0.039
Percent of Type IIb Fibers	59.0 ± 22.9	22.8 ± 10.1 *	50.7 ± 8.5	0.016
Percent of Type IIx Fibers	16.6 ± 2.3	18.6 ± 4.2	13.0 ± 3.6	0.574
Data analyzed by one-way ANOVA, presented as mean ± SD. Different than *control				

(p<0.001). A main effect of fiber type was also observed, whereby type IIb fibers were larger than type I, IIa, and IIx fibers, and type IIx fibers were larger than type I and IIa fibers (all p<0.001; **Figure 6B**). When mean proportions were compared, there was a significant interaction between group and fiber type (p<0.001), where

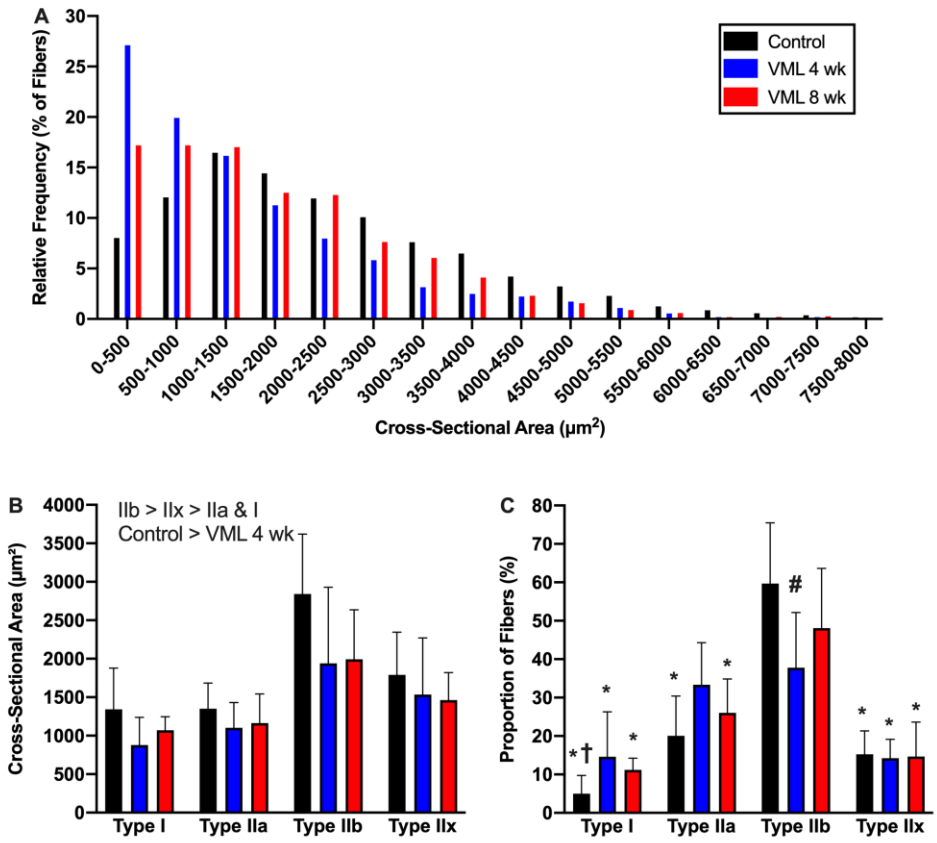

Figure 6: Fiber type specific differences in the gastrocnemius muscles were evaluated up to 8-weeks following VML**. A)** The distribution of muscle fiber cross-sectional area (CSA) in controls was normally distributed at 1,000-1,500μm² with a slight right skew. Compared to control, the distribution of muscle fiber cross-sectional area shifted left at 4- and 8-weeks post VML (p<0.001), but VML groups were not different than each other (p<0.017). **B)** Overall muscle fiber CSA was smaller at 4-weeks post-VML compared to control (main effect experimental group; p=0.011). As expected, type IIb fibers had a greater CSA than type I, IIa, and IIx; additionally type IIx fibers were larger than type I and IIa fibers (main effect of fiber type; p<0.001). **C)** There was a significant interaction (group x fiber type; p=0.001) in the proportion of fiber types across the gastrocnemius muscle. Specifically muscles post-VML had a higher proportion of type IIb fibers compared to type I and IIx at 4-weeks, and type I, IIa, and IIx at 8-weeks; and control muscles generally demonstrated a greater proportion of type IIb fibers compared to type I, IIa, and IIx, and compared to type IIb fibers of muscles 4-weeks post-VML. Data presented as mean±SD; analyzed by chi-squared and two-way ANOVA, significant main effects are indicated within figure. Within experimental group, significantly different from *type IIb; †type IIa. Within fiber type, significantly different from #control.

type I, IIx, and IIa were the least represented, and type IIb was the most represented. Compared to control, VML groups tended to have greater expression of type I and IIa fibers, and lower type IIb, particularly at 4 weeks (**Figure 6C**). Interestingly, muscle fiber type proportions were not significantly different within the mid-region bordering the VML injury ($p \geq 0.234$). In contrast, at 4-weeks post-VML, the proportion of type I and IIa muscle fibers increased substantially while the proportion of type IIb fibers decreased in the medial gastrocnemius ($p \leq 0.039$; **Table 6**). By 8-weeks post-VML, regional differences in fiber type proportion diminished, except for an increase in the proportion of type I fibers in the lateral gastrocnemius ($p=0.012$).

DISCUSSION

The pathophysiologic comorbidities of VML injury are vast and range from functional deficits, impaired inflammatory signaling, and chronic fibrotic deposition. However, to date both muscle-specific and whole-body understanding of the metabolic consequences of VML injury are incompletely understood, in both animal models and the patient population. The primary finding in this work is that even with a relatively small volume of the total body skeletal muscle lost to VML injury, there are local and whole-body impairments to metabolism. Whole-body metabolism alterations seem to be largely due to changes in carbohydrate utilization that occur during active hours, rather than reductions in physical activity overall.

Following VML injury, less carbohydrates and more lipids were utilized per unit of physical activity. This finding may indicate metabolic inflexibility, which is the inability to transition effectively between carbohydrate and lipid utilization [125]. Metabolic inflexibility, precedes various disorders, placing the organism at greater risk for comorbidities. Sedentarism often occurs following orthopaedic injury [83–85], which in turn, increases the risk of metabolic inflexibility and additional comorbidities such as obesity, type II diabetes, heart disease, and osteoporosis [87]. Previous work [98,108] and this study, indicate that physical activity levels

may not decrease following VML injury, yet herein, metabolic impairment still occurred. This supports that mitochondrial dysfunction in VML-injured muscle may drive whole body metabolic impairment as a primary outcome of VML injury, a previously unreported finding with significant comorbidity implications.

Following VML injury, physical activity was not reduced despite a substantial loss of force generating capacity. The force loss associated with VML injury is primarily due to an indiscriminate loss of contractile tissue in addition to a one of many secondary losses due to axotomy, as observed previously in VML injury [102]. Axotomy indicates denervation, which has been shown to increase representation of slow muscle fibers and decrease representation of fast fibers across the muscle in a denervation specific model [64]. A similar shift in fiber type was observed acutely within this study, supporting that some of the fiber type changes observed post-VML may be caused by axotomy. A shift to slower fiber type across the muscle may signify a preference to preserve low force function, such as ambulation, while sacrificing maximal force generation. Limiting force may serve to protect the muscle from damaging, high-force contractions during the early wound healing phase. However, impairments to force generation persisted chronically and there appeared to be little or no overall improvement to oxidative function despite an apparent preference to conserve oxidative muscle fibers.

Although oxidative muscle fibers were conserved, the oxidative potential of the muscle was not improved, as evidenced by a decrease in capillarity and no change in most measures of mitochondrial enzyme activity and content. An increase inmetabolic activity, as evidenced by an increase in NADH expression was observed, but may indicate mitochondrial dysregulation rather than positive adaptation. An increase in mitochondrial activity without an improvement in contractile or metabolic function may indicate that mitochondrial function is impaired following VML. . It is likely that mitochondrial dysregulation underlies pathologic outcomes following VML injury, a concept that is corroborated by previous work. Specifically, mitochondrial dysregulation occurs post VML injury, which presents as reduced oxidative capacity and increased ROS generation

compared to uninjured muscle [98,107,116]. Mitochondrial dysregulation also occurs in other conditions besides VML, including denervation [66,67], burn [60], and immobilization [90]. Normally, metabolic outcomes improve over time once regeneration, mobilization, and rehabilitation occur. In contrast, mobilization and rehabilitation following VML injury is not sufficient to attenuate metabolic impairment [126], and regeneration is currently not possible.

Failure in regenerative mechanisms is of primary concern in VML injury and complicates therapeutic efforts post-injury. Within this study, the acute and chronic increase in centrally located nuclei support that the intramuscular environment is unstable long past the time of injury. It is likely that early wound healing processes, such as fibrotic deposition [106,127,128] are prioritized, impairing the capacity of the muscle to adapt positively to physical activity or rehabilitation. Compounding this, the acute decline in capillary distribution indicates that the muscular environment may have lower blood supply, which may inhibit beneficial adaptation and functional capacity. Capillarity did not return to normal until 8-weeks post-injury, which also aligns with a return to pre-injury levels of complex I activity, fiber type proportion, and size distribution. For conditions like burn [63], critical illness [129], and traumatic injury [130] early mobilization is recommended and generally improves outcomes. However, in cases of VML injury the underlying pathophysiology may resist the benefits of early rehabilitation, necessitating further attention to address metabolic impairment early chronically in treatment.

In conclusion, metabolic inflexibility occurred following VML injury as a primary outcome, largely due to reductions in carbohydrate utilization at the whole-body level. Though it was hypothesized that reductions in physical activity would drive metabolic impairment, the pathophysiology of VML injury was sufficient to cause metabolic inflexibility without a change in physical activity. This finding may indicate a need to treat metabolic disorder, as even if recommended levels of physical activity are met, metabolic impairment may still occur, increasing the risk for metabolic comorbidity. Further assessment of the muscle remaining after injury revealed an overall reduction in fast twitch muscle while conserving slower,

oxidative fibers. The slowing of the muscle may be protective, preventing damaging force generation during wound healing, however force loss persists in VML, leaving the injured limb disabled chronically. Additionally, it is possible that reduced capillary support contributes to poor functional outcomes post-injury by limiting perfusion to the site of injury. In sum, regenerative and rehabilitative strategies will need to address functional and metabolic pathophysiologic changes early post injury, and failure to do so may increase the risk for whole body metabolic impairments and comorbidity.

Chapter 3: Conclusions and Future Directions

The findings from this work provide a novel insight into the complex inner workings of the pathophysiology of VML injury and how it affects the organism as a whole. Following VML injury, the loss of contractile tissue impairs force generation of the effected muscle. In some regards, limiting force generation may be protective during the early stages of wound healing, both preventing excessive force generation and preserving low force function. However, force loss is not recoverable in VML injury, impairing the overall function of the affected limb. Alongside loss of force, intramuscular metabolism appears to shift towards an oxidative preference, maintaining oxidative fibers while losing glycolytic. This relationship is also observed following denervation [64], and may support that some of the pathophysiologic outcomes of VML injury may be directly caused by motor neuron axotomy, which has been observed in VML injury [102].

Despite a shift towards oxidative fibers, whole body oxidative function actually decreased over time, as evidenced by a whole-body reduction in metabolic rate and RER. Metabolic impairment may be explained in part by dysfunction in skeletal muscle specific mitochondria, which has been observed in various muscle injuries, including denervation [67] and burn [60], as well as in VML injury [98]. While the exact link between VML injury and whole-body metabolic impairment is not yet clear, it is possible that damage to the muscle and surrounding structures may cause an effect systemically. Damage to the mitochondrial and capillary networks in VML injury may allow release of mitochondrial fragments into circulation, which may increase inflammatory signaling [95]. Inflammation has been linked to metabolic impairments in various diseases and conditions, including muscular dystrophy and critical illness. Though different in etiology than VML, muscular dystrophy may have some similarities that help to explain some of the whole-body metabolic dysfunction post-VML injury. In muscular dystrophy, impairments to the muscle membrane results in atrophy and fibrosis, leading to cycles of degeneration and regeneration, increases in centrally located nuclei, and systemic inflammation [78,79]. Similarly, atrophy and fibrosis occur post-VML, along with increases in centrally located nuclei and inflammation. It is possible that systemic inflammation

occurs after VML injury, resulting in blunted glucose metabolism. Further work will need to elucidate if inflammation is the link between VML-injury and whole-body metabolic impairment, and treatment may need to address pathophysiologic changes to the muscle alongside of treatment at the whole-body level.

VML injury presents a unique and difficult challenge to regenerative and rehabilitative approaches. Ideally, regeneration of the lost muscle following VML injury would improve both function of the limb and mitigate whole body metabolic disorder. However, no regenerative treatment to date has been able to induce substantial *de novo* muscle fiber regeneration post-VML, nor has any rehabilitative method been able to fully restore force loss [100,115,126]. As regeneration is currently unobtainable, improving the remaining muscle plasticity may be a viable option to improve both acute and chronic outcomes post-VML. Reduced plasticity of the injured muscle is a known barrier to both regenerative and rehabilitative efforts [126], therefore, reinstating muscle responsiveness will be a critical aspect of treatment efforts. This may prove especially important as the patient ages, as age related declines to muscle and mitochondria may worsen outcomes long-term. Translational research has had some success with restoring plasticity to VML injured muscle through PGC-1α overexpression [98], but it is unknown if such an improvement can prevent whole-body metabolic impairment. Additionally, transgenic overexpression of PGC-1α is not viable for human treatment, therefore using other mitochondrial therapies may be necessary. For example, pyrroloquinoline quinone has been utilized to improve mitochondrial function following denervation [64], but it is unknown if similar effects may occur in humans or following VML injury.

Some rehabilitative benefits have been observed following VML injury [108,116], however the effects are very limited when compared to uninjured muscle. There is a possibility that restoring muscle plasticity in combination with rehabilitation may be able to augment outcomes further than either paradigm alone, allowing improvements in metabolic function. However more work will need to be conducted on combinatorial therapies to support clinical application. Still, it

is unlikely that even a combination of therapies will be successful in fully overcoming the overwhelming pathology presented by VML injury. As future work aims towards solving VML, consideration for chronic care needs to be taken seriously as relatively small loses in muscle tissue may have the potential to impair metabolic outcomes on the full body level, even if physical activity is maintained, which this work has pointed out.

References

[1] Janssen, I., Heymsfield, S.B., Wang, Z., and Ross, R. (2000) Skeletal muscle mass and distribution in 468 men and women aged 18–88 yr. *Journal of Applied Physiology*. 89 (1), 81–88.

[2] Frontera, W.R. and Ochala, J. (2015) Skeletal Muscle: A Brief Review of Structure and Function. *Calcified Tissue International*. 96 (3), 183–195.

[3] Hall, Z.W. and Ralston, E. (1989) Nuclear domains in muscle cells. *Cell*. 59 (5), 771–772.

[4] Kjaer, M. (2004) Role of extracellular matrix in adaptation of tendon and skeletal muscle to mechanical loading. *Physiological Reviews*. 84 (2), 649–698.

[5] Clark, K.A., McElhinny, A.S., Beckerle, M.C., and Gregorio, C.C. (2002) Striated Muscle Cytoarchitecture: An Intricate Web of Form and Function. *Annual Review of Cell and Developmental Biology*. 18 (1), 637–706.

[6] Franchi, M.V., Reeves, N.D., and Narici, M.V. (2017) Skeletal Muscle Remodeling in Response to Eccentric vs. Concentric Loading: Morphological, Molecular, and Metabolic Adaptations. *Frontiers in Physiology*. 8 447.

[7] Morgan, J.E. and Partridge, T.A. (2003) Muscle satellite cells. *The International Journal of Biochemistry & Cell Biology*. 35 (8), 1151–1156.

[8] Bruusgaard, J.C., Liestøl, K., Ekmark, M., Kollstad, K., and Gundersen, K. (2003) Number and spatial distribution of nuclei in the muscle fibres of normal mice studied in vivo. *The Journal of Physiology*. 551 (Pt 2), 467–478.

[9] Murach, K.A., Englund, D.A., Dupont-Versteegden, E.E., McCarthy, J.J., and Peterson, C.A. (2018) Myonuclear Domain Flexibility Challenges Rigid Assumptions on Satellite Cell Contribution to Skeletal Muscle Fiber Hypertrophy. *Frontiers in Physiology*. 9.

[10] Asfour, H.A., Allouh, M.Z., and Said, R.S. (2018) Myogenic regulatory factors: The orchestrators of myogenesis after 30 years of discovery. *Experimental Biology and Medicine*. 243 (2), 118–128.

[11] Kuang, S., Kuroda, K., Le Grand, F., and Rudnicki, M.A. (2007) Asymmetric Self-Renewal and Commitment of Satellite Stem Cells in Muscle. *Cell*. 129 (5), 999–1010.

[12] McCarthy, J.J., Mula, J., Miyazaki, M., Erfani, R., Garrison, K., Farooqui, A.B., et al. (2011) Effective fiber hypertrophy in satellite cell-depleted skeletal muscle. *Development*. 138 (17), 3657–3666.

[13] Adams, G.R. (2006) Satellite cell proliferation and skeletal muscle hypertrophy. *Applied Physiology, Nutrition, and Metabolism*. 31 (6), 782–790.

[14] Murach, K.A., Fry, C.S., Kirby, T.J., Jackson, J.R., Lee, J.D., White, S.H., et al. (2018) Starring or Supporting Role? Satellite Cells and Skeletal Muscle Fiber Size Regulation. *Physiology*. 33 (1), 26–38.

[15] Thomas, H.M., Cowin, A.J., and Mills, S.J. (2017) The Importance of Pericytes in Healing: Wounds and other Pathologies. *International Journal of Molecular Sciences*. 18 (6),.
[16] Wong, S.-P., Rowley, J.E., Redpath, A.N., Tilman, J.D., Fellous, T.G., and Johnson, J.R. (2015) Pericytes, mesenchymal stem cells and their contributions to tissue repair. *120*.
[17] König, M.A., Canepa, D.D., Cadosch, D., Casanova, E., Heinzelmann, M., Rittirsch, D., et al. (2016) Direct transplantation of native pericytes from adipose tissue: A new perspective to stimulate healing in critical size bone defects. *Cytotherapy*. 18 (1), 41–52.
[18] Dellavalle, A., Maroli, G., Covarello, D., Azzoni, E., Innocenzi, A., Perani, L., et al. (2011) Pericytes resident in postnatal skeletal muscle differentiate into muscle fibres and generate satellite cells. *Nature Communications*. 2 499.
[19] Figueiredo, V.C. and McCarthy, J.J. (2018) Regulation of Ribosome Biogenesis in Skeletal Muscle Hypertrophy. *Physiology*. 34 (1), 30–42.
[20] Zachar, I. and Szathmáry, E. (2017) Breath-giving cooperation: critical review of origin of mitochondria hypotheses. *Biology Direct*. 12.
[21] Picca, A., Lezza, A.M.S., Leeuwenburgh, C., Pesce, V., Calvani, R., Bossola, M., et al. (2018) Circulating Mitochondrial DNA at the Crossroads of Mitochondrial Dysfunction and Inflammation During Aging and Muscle Wasting Disorders. *Rejuvenation Research*. 21 (4), 350–359.
[22] Cannavino, J., Brocca, L., Sandri, M., Grassi, B., Bottinelli, R., and Pellegrino, M.A. (2015) The role of alterations in mitochondrial dynamics and PGC-1α over-expression in fast muscle atrophy following hindlimb unloading. *The Journal of Physiology*. 593 (8), 1981–1995.
[23] Lee, H. and Yoon, Y. (2016) Mitochondrial fission and fusion. *Biochemical Society Transactions*. 44 (6), 1725–1735.
[24] Perry, C.G.R. and Hawley, J.A. (2018) Molecular Basis of Exercise-Induced Skeletal Muscle Mitochondrial Biogenesis: Historical Advances, Current Knowledge, and Future Challenges. *Cold Spring Harbor Perspectives in Medicine*. 8 (9), a029686.
[25] Buller, A.J., Eccles, J.C., and Eccles, R.M. (1960) Interactions between motoneurones and muscles in respect of the characteristic speeds of their responses. *The Journal of Physiology*. 150 (2), 417–439.
[26] Burke, R.E. and Edgerton, V.R. (1975) Motor Unit Properties and Selective Involvement In Movement. *Exercise and Sport Sciences Reviews*. 3 (1), 31.
[27] Bottinelli, R. and Reggiani, C. (2000) Human skeletal muscle fibres: molecular and functional diversity. *Progress in Biophysics and Molecular Biology*. 73 (2), 195–262.
[28] Bottinelli, R., Betto, R., Schiaffino, S., and Reggiani, C. (1994) Maximum shortening velocity and coexistence of myosin heavy chain isoforms in single skinned fast fibres of rat skeletal muscle. *Journal of Muscle Research and Cell Motility*. 15 (4), 413–419.

[29] Billeter, R., Heizmann, C.W., Howald, H., and Jenny, E. (1981) Analysis of Myosin Light and Heavy Chain Types in Single Human Skeletal Muscle Fibers. *European Journal of Biochemistry*. 116 (2), 389–395.
[30] Greising, S.M., Gransee, H.M., Mantilla, C.B., and Sieck, G.C. (2012) Systems Biology of Skeletal Muscle: Fiber Type as an Organizing Principle. *Wiley Interdisciplinary Reviews. Systems Biology and Medicine*. 4 (5),.
[31] Ferraro, E., Giammarioli, A.M., Chiandotto, S., Spoletini, I., and Rosano, G. (2014) Exercise-Induced Skeletal Muscle Remodeling and Metabolic Adaptation: Redox Signaling and Role of Autophagy. *Antioxidants & Redox Signaling*. 21 (1), 154–176.
[32] Gollnick, P.D., Sjödin, B., Karlsson, J., Jansson, E., and Saltin, B. (1974) Human soleus muscle: A comparison of fiber composition and enzyme activities with other leg muscles. *Pflügers Archiv European Journal of Physiology*. 348 (3), 247–255.
[33] Zierath, J.R. and Hawley, J.A. (2004) Skeletal Muscle Fiber Type: Influence on Contractile and Metabolic Properties. *PLoS Biology*. 2 (10),.
[34] Cuevas, J. (2007) The Somatic Nervous System. in: S.J. Enna, D.B. Bylund (Eds.), XPharm Compr. Pharmacol. Ref., Elsevier, New Yorkpp. 1–13.
[35] Feinstein, B., Lindegård, B., Nyman, E., and Wohlfart, G. (1955) MORPHOLOGIC STUDIES OF MOTOR UNITS IN NORMAL HUMAN MUSCLES. *Cells Tissues Organs*. 23 (2), 127–142.
[36] Remington, L.A. (2012) Clinical anatomy and physiology of the visual system. 3rd ed.. Elsevier/Butterworth-Heinemann, St. Louis, Mo.
[37] Burke, R.E. and Edgerton, V.R. (1975) Motor Unit Properties and Selective Involvement In Movement. *Exercise & Sport Sciences Reviews*. 3 (1), 31–82.
[38] Chamberlain, S. and Lewis, D.M. (1989) Contractile characteristics and innervation ratio of rat soleus motor units. *The Journal of Physiology*. 412 1–21.
[39] Burke, R.E. and Tsairis, P. (1973) Anatomy and innervation ratios in motor units of cat gastrocnemius. *The Journal of Physiology*. 234 (3), 749–765.
[40] Henneman, E. (1957) Relation between Size of Neurons and Their Susceptibility to Discharge. *Science*. 126 (3287), 1345–1347.
[41] Bers, D.M. (2014) 16 - Excitation-Contraction Coupling. in: D.P. Zipes, J. Jalife (Eds.), Card. Electrophysiol. Cell Bedside Sixth Ed., W.B. Saunders, Philadelphiapp. 161–169.
[42] Anthony, T.G. (2016) Mechanisms of protein balance in skeletal muscle. *Domestic Animal Endocrinology*. 56 (Suppl), S23–S32.
[43] Tipton, K.D., Hamilton, D.L., and Gallagher, I.J. (2018) Assessing the Role of Muscle Protein Breakdown in Response to Nutrition and Exercise in Humans. *Sports Medicine (Auckland, N.Z.)*. 48 (Suppl 1), 53–64.
[44] Rennie, M.J., Bohé, J., Smith, K., Wackerhage, H., and Greenhaff, P. (2006) Branched-Chain Amino Acids as Fuels and Anabolic Signals in Human Muscle. *The Journal of Nutrition*. 136 (1), 264S-268S.

[45] Richter, E.A. and Hargreaves, M. (2013) Exercise, GLUT4, and Skeletal Muscle Glucose Uptake. *Physiological Reviews*. 93 (3), 993–1017.
[46] Bharat, T.A.M., Malsam, J., Hagen, W.J.H., Scheutzow, A., Söllner, T.H., and Briggs, J.A.G. (2014) SNARE and regulatory proteins induce local membrane protrusions to prime docked vesicles for fast calcium-triggered fusion. *EMBO Reports*. 15 (3), 308–314.
[47] Robergs, R.A., Ghiasvand, F., and Parker, D. (2004) Biochemistry of exercise-induced metabolic acidosis. *American Journal of Physiology. Regulatory, Integrative and Comparative Physiology*. 287 (3), R502-516.
[48] Krebs, H.A. and Kornberg, H.L. (1957) Energy Transformations in Living Matter. in: H.A. Krebs, H.L. Kornberg (Eds.), Energy Transform. Living Matter Surv., Springer, Berlin, Heidelbergpp. 212–298.
[49] Morales, P.E., Bucarey, J.L., and Espinosa, A. (2017) Muscle Lipid Metabolism: Role of Lipid Droplets and Perilipins. *Journal of Diabetes Research*. 2017.
[50] Kennedy, M.A. (2010) A Brief Review of the Basics of Immunology: The Innate and Adaptive Response. *Veterinary Clinics of North America: Small Animal Practice*. 40 (3), 369–379.
[51] Zhou, D., Huang, C., Lin, Z., Zhan, S., Kong, L., Fang, C., et al. (2014) Macrophage polarization and function with emphasis on the evolving roles of coordinated regulation of cellular signaling pathways. *Cellular Signalling*. 26 (2), 192–197.
[52] Giordani, L., Parisi, A., and Le Grand, F. (2018) Chapter Six - Satellite Cell Self-Renewal. in: D. Sassoon (Ed.), Curr. Top. Dev. Biol., Academic Press, pp. 177–203.
[53] Tidball, J.G. (2011) Mechanisms of muscle injury, repair, and regeneration. *Comprehensive Physiology*. 1 (4), 2029–2062.
[54] Tierney, M.T. and Sacco, A. (2016) Inducing and Evaluating Skeletal Muscle Injury by Notexin and Barium Chloride. in: M. Kyba (Ed.), Skelet. Muscle Regen. Mouse Methods Protoc., Springer New York, New York, NYpp. 53–60.
[55] Lefaucheur, J.P. and Sébille, A. (1995) The cellular events of injured muscle regeneration depend on the nature of the injury. *Neuromuscular Disorders*. 5 (6), 501–509.
[56] Forouhar, F., Huang, W.-N., Liu, J.-H., Chien, K.-Y., Wu, W., and Hsiao, C.-D. (2003) Structural basis of membrane-induced cardiotoxin A3 oligomerization. *The Journal of Biological Chemistry*. 278 (24), 21980–21988.
[57] Hardy, D., Besnard, A., Latil, M., Jouvion, G., Briand, D., Thépenier, C., et al. (2016) Comparative Study of Injury Models for Studying Muscle Regeneration in Mice. *PLoS ONE*. 11 (1),.
[58] Lapa, A.J., Albuquerque, E.X., and Daly, J. (1974) An electrophysiological study of the effects of D-tubocurarine, atropine, and alpha-bungarotoxin on the cholinergic receptor in innervated and chronically denervated mammalian skeletal muscles. *Experimental Neurology*. 43 (2), 375–398.

[59] Williams, F.N. and Herndon, D.N. (2017) Metabolic and Endocrine Considerations After Burn Injury. *Clinics in Plastic Surgery*. 44 (3), 541–553.
[60] Porter, C., Herndon, D.N., Børsheim, E., Bhattarai, N., Chao, T., Reidy, P.T., et al. (2016) Long-Term Skeletal Muscle Mitochondrial Dysfunction is Associated with Hypermetabolism in Severely Burned Children. *Journal of Burn Care & Research: Official Publication of the American Burn Association*. 37 (1), 53–63.
[61] Rontoyanni, V.G., Malagaris, I., Herndon, D.N., Rivas, E., Capek, K.D., Delgadillo, A.D., et al. (2018) Skeletal Muscle Mitochondrial Function is Determined by Burn Severity, Sex, and Sepsis, and is Associated With Glucose Metabolism and Functional Capacity in Burned Children. *Shock (Augusta, Ga.)*. 50 (2), 141–148.
[62] Porter, C., Herndon, D.N., Bhattarai, N., Ogunbileje, J.O., Szczesny, B., Szabo, C., et al. (2016) Differential acute and chronic effects of burn trauma on murine skeletal muscle bioenergetics. *Burns : Journal of the International Society for Burn Injuries*. 42 (1), 112–122.
[63] Porter, C., Hardee, J., Herndon, D.N., and Suman, O.E. (2015) The role of exercise in the rehabilitation of patients with severe burns. *Exercise and Sport Sciences Reviews*. 43 (1), 34–40.
[64] Kuo, Y.-T., Shih, P.-H., Kao, S.-H., Yeh, G.-C., and Lee, H.-M. (2015) Pyrroloquinoline Quinone Resists Denervation-Induced Skeletal Muscle Atrophy by Activating PGC-1α and Integrating Mitochondrial Electron Transport Chain Complexes. *PLoS ONE*. 10 (12),.
[65] Tryon, L.D., Crilly, M.J., and Hood, D.A. (2015) Effect of denervation on the regulation of mitochondrial transcription factor A expression in skeletal muscle. *American Journal of Physiology-Cell Physiology*. 309 (4), C228–C238.
[66] Adhihetty, P.J., O'Leary, M.F.N., Chabi, B., Wicks, K.L., and Hood, D.A. (2007) Effect of denervation on mitochondrially mediated apoptosis in skeletal muscle. *Journal of Applied Physiology*. 102 (3), 1143–1151.
[67] O′Leary, M.F.N., Vainshtein, A., Carter, H.N., Zhang, Y., and Hood, D.A. (2012) Denervation-induced mitochondrial dysfunction and autophagy in skeletal muscle of apoptosis-deficient animals. *American Journal of Physiology-Cell Physiology*. 303 (4), C447–C454.
[68] Singh, K. and Hood, D.A. (2011) Effect of denervation-induced muscle disuse on mitochondrial protein import. *American Journal of Physiology. Cell Physiology*. 300 (1), C138-145.
[69] Stefancic, M., Vidmar, G., and Blagus, R. (2016) Long-term recovery of muscle strength after denervation in the fibular division of the sciatic nerve. *Muscle & Nerve*. 54 (4), 702–708.
[70] Lodeserto, F. and Yende, S. (2014) Understanding skeletal muscle wasting in critically ill patients. *Critical Care*. 18 (6),.

[71] Bolton, C.F., Gilbert, J.J., Hahn, A.F., and Sibbald, W.J. (1984) Polyneuropathy in critically ill patients. *Journal of Neurology, Neurosurgery, and Psychiatry*. 47 (11), 1223–1231.
[72] Zhou, C., Wu, L., Ni, F., Ji, W., Wu, J., and Zhang, H. (2014) Critical illness polyneuropathy and myopathy: a systematic review. *Neural Regeneration Research*. 9 (1), 101–110.
[73] Schmidt, C.A., Ryan, T.E., Lin, C.-T., Inigo, M.M.R., Green, T.D., Brault, J.J., et al. (2017) Diminished force production and mitochondrial respiratory deficits are strain-dependent myopathies of subacute limb ischemia. *Journal of Vascular Surgery*. 65 (5), 1504-1514.e11.
[74] van den Berg, M., Hooijman, P.E., Beishuizen, A., de Waard, M.C., Paul, M.A., Hartemink, K.J., et al. (2017) Diaphragm Atrophy and Weakness in the Absence of Mitochondrial Dysfunction in the Critically Ill. *American Journal of Respiratory and Critical Care Medicine*. 196 (12), 1544–1558.
[75] Graul, A.I., Stringer, M., and Sorbera, L. (2016) Cachexia. *Drugs of Today*. 52 (9), 519.
[76] Brown, J.L., Rosa-Caldwell, M.E., Lee, D.E., Blackwell, T.A., Brown, L.A., Perry, R.A., et al. (2017) Mitochondrial degeneration precedes the development of muscle atrophy in progression of cancer cachexia in tumour-bearing mice. *Journal of Cachexia, Sarcopenia and Muscle*. 8 (6), 926–938.
[77] Griffiths, R.D. and Hall, J.B. (2010) Intensive care unit-acquired weakness. *Critical Care Medicine*. 38 (3), 779–787.
[78] Dalkilic, I. and Kunkel, L.M. (2003) Muscular dystrophies: genes to pathogenesis. *Current Opinion in Genetics & Development*. 13 (3), 231–238.
[79] Guzmán, O. del R.C., García, A.L.C., and Rodríguez-Cruz, M. (2012) Muscular Dystrophies at Different Ages: Metabolic and Endocrine Alterations. *International Journal of Endocrinology*. 2012.
[80] Desguerre, I., Mayer, M., Leturcq, F., Barbet, J.-P., Gherardi, R.K., and Christov, C. (2009) Endomysial fibrosis in Duchenne muscular dystrophy: a marker of poor outcome associated with macrophage alternative activation. *Journal of Neuropathology and Experimental Neurology*. 68 (7), 762–773.
[81] Zanotti, S., Saredi, S., Ruggieri, A., Fabbri, M., Blasevich, F., Romaggi, S., et al. (2007) Altered extracellular matrix transcript expression and protein modulation in primary Duchenne muscular dystrophy myotubes. *Matrix Biology*. 26 (8), 615–624.
[82] de Greef, J.C., Hamlyn, R., Jensen, B.S., O'Campo Landa, R., Levy, J.R., Kobuke, K., et al. (2016) Collagen VI deficiency reduces muscle pathology, but does not improve muscle function, in the γ-sarcoglycan-null mouse. *Human Molecular Genetics*. 25 (7), 1357–1369.
[83] Zusman, E.Z., Dawes, M.G., Edwards, N., and Ashe, M.C. (2018) A systematic review of evidence for older adults' sedentary behavior and physical activity after hip fracture. *Clinical Rehabilitation*. 32 (5), 679–691.

[84] Stubbs, C.O. and Lee, A.J. (2004) The obesity epidemic: both energy intake and physical activity contribute. *The Medical Journal of Australia*. 181 (9), 489–491.
[85] Ceroni, D., Martin, X., Delhumeau, C., and Farpour-Lambert, N. (2011) Decrease of physical activity level in adolescents with limb fractures: an accelerometry-based activity monitor study. *BMC Musculoskeletal Disorders*. 12 87.
[86] Maggio, A.B., Martin, X.E., and Ceroni, D. (2017) Activity-related energy expenditure during lower limb cast immobilization in children. *Journal of Pediatric Orthopedics. Part B*. 26 (3), 217–221.
[87] Booth, F.W. and Hargreaves, M. (2011) Understanding multi-organ pathology from insufficient exercise. *Journal of Applied Physiology*. 111 (4), 1199–1200.
[88] Kelley, D.E. and Mandarino, L.J. (2000) Fuel selection in human skeletal muscle in insulin resistance: a reexamination. *Diabetes*. 49 (5), 677–683.
[89] Irimia, J.M., Guerrero, M., Rodriguez-Miguelez, P., Cadefau, J.A., Tesch, P.A., Cussó, R., et al. (2017) Metabolic adaptations in skeletal muscle after 84 days of bed rest with and without concurrent flywheel resistance exercise. *Journal of Applied Physiology (Bethesda, Md.: 1985)*. 122 (1), 96–103.
[90] Kang, C. and Ji, L.L. (2013) Muscle immobilization and remobilization downregulates PGC-1α signaling and the mitochondrial biogenesis pathway. *Journal of Applied Physiology*. 115 (11), 1618–1625.
[91] Sehl, M.E. and Yates, F.E. (2001) Kinetics of Human AgingI. Rates of Senescence Between Ages 30 and 70 Years in Healthy People. *The Journals of Gerontology: Series A*. 56 (5), B198–B208.
[92] Barnouin, Y., McPhee, J.S., Butler-Browne, G., Bosutti, A., De Vito, G., Jones, D.A., et al. (2017) Coupling between skeletal muscle fiber size and capillarization is maintained during healthy aging. *Journal of Cachexia, Sarcopenia and Muscle*. 8 (4), 647–659.
[93] Joseph, A.-M., Adhihetty, P.J., Buford, T.W., Wohlgemuth, S.E., Lees, H.A., Nguyen, L.M.-D., et al. (2012) The Impact of Aging on Mitochondrial Function and Biogenesis Pathways in Skeletal Muscle of Sedentary High- and Low-Functioning Elderly Individuals. *Aging Cell*. 11 (5), 801–809.
[94] Hyatt, H., Deminice, R., Yoshihara, T., and Powers, S.K. (2019) Mitochondrial dysfunction induces muscle atrophy during prolonged inactivity: A review of the causes and effects. *Archives of Biochemistry and Biophysics*. 662 49–60.
[95] Zhang, Q., Raoof, M., Chen, Y., Sumi, Y., Sursal, T., Junger, W., et al. (2010) Circulating mitochondrial DAMPs cause inflammatory responses to injury. *Nature*. 464 (7285), 104–107.
[96] Pollot, B.E. and Corona, B.T. (2016) Volumetric Muscle Loss. in: M. Kyba (Ed.), Skelet. Muscle Regen. Mouse Methods Protoc., Springer, New York, NYpp. 19–31.

[97] Corona, B.T., Wenke, J.C., and Ward, C.L. (2016) Pathophysiology of Volumetric Muscle Loss Injury. *Cells Tissues Organs*. 202 (3–4), 180–188.
[98] Southern, W.M., Nichenko, A.S., Tehrani, K.F., McGranahan, M.J., Krishnan, L., Qualls, A.E., et al. (2019) PGC-1α overexpression partially rescues impaired oxidative and contractile pathophysiology following volumetric muscle loss injury. *Scientific Reports*. 9.
[99] Greising, S.M., Corona, B.T., McGann, C., Frankum, J.K., and Warren, G.L. (2019) Therapeutic Approaches for Volumetric Muscle Loss Injury: A Systematic Review and Meta-Analysis. *Tissue Engineering Part B: Reviews*. 25 (6), 510–525.
[100] Corona, B.T., Rivera, J.C., Owens, J.G., Wenke, J.C., and Rathbone, C.R. (2015) Volumetric muscle loss leads to permanent disability following extremity trauma. *Journal of Rehabilitation Research and Development*. 52 (7), 785–792.
[101] (2014) United States Bone and Joint Initiative: The Burden of Musculoskeletal Diseases in the United States (BMUS). *BMUS: The Burden of Musculoskeletal Diseases in the United States*.
[102] Corona, B.T., Flanagan, K.E., Brininger, C.M., Goldman, S.M., Call, J.A., and Greising, S.M. (2018) Impact of volumetric muscle loss injury on persistent motoneuron axotomy. *Muscle & Nerve*. 57 (5), 799–807.
[103] Carlson, B.M. (2014) The Biology of Long-Term Denervated Skeletal Muscle. *European Journal of Translational Myology*. 24 (1), 3293.
[104] Hurtgen, B.J., Ward, C.L., Garg, K., Pollot, B.E., Goldman, S.M., McKinley, T.O., et al. (2016) Severe muscle trauma triggers heightened and prolonged local musculoskeletal inflammation and impairs adjacent tibia fracture healing. *Journal of Musculoskeletal & Neuronal Interactions*. 16 (2), 122–134.
[105] Evano, B. and Tajbakhsh, S. (2018) Skeletal muscle stem cells in comfort and stress. *NPJ Regenerative Medicine*. 3.
[106] Corona, B.T., Rivera, J.C., Dalske, K.A., Wenke, J.C., and Greising, S.M. (2020) Pharmacological Mitigation of Fibrosis in a Porcine Model of Volumetric Muscle Loss Injury. *Tissue Engineering. Part A*.
[107] Chao, T., Burmeister, D.M., Corona, B.T., and Greising, S.M. (2019) Oxidative pathophysiology following volumetric muscle loss injury in a porcine model. *Journal of Applied Physiology*. 126 (6), 1541–1549.
[108] Aurora, A., Garg, K., Corona, B.T., and Walters, T.J. (2014) Physical rehabilitation improves muscle function following volumetric muscle loss injury. *BMC Sports Science, Medicine and Rehabilitation*. 6.
[109] van Loon, L.J.C., Greenhaff, P.L., Constantin-Teodosiu, D., Saris, W.H.M., and Wagenmakers, A.J.M. (2001) The effects of increasing exercise intensity on muscle fuel utilisation in humans. *The Journal of Physiology*. 536 (Pt 1), 295–304.
[110] Dagenais, G.R., Tancredi, R.G., and Zierler, K.L. (1976) Free fatty acid oxidation by forearm muscle at rest, and evidence for an intramuscular lipid

pool in the human forearm. *The Journal of Clinical Investigation*. 58 (2), 421–431.
[111] Goodpaster, B.H. and Sparks, L.M. (2017) Metabolic flexibility in health and disease. *Cell Metabolism*. 25 (5), 1027–1036.
[112] Goodpaster, B.H. and Sparks, L.M. (2017) Metabolic Flexibility in Health and Disease. *Cell Metabolism*. 25 (5), 1027–1036.
[113] Rynders, C.A., Blanc, S., DeJong, N., Bessesen, D.H., and Bergouignan, A. (2018) Sedentary behaviour is a key determinant of metabolic inflexibility. *The Journal of Physiology*. 596 (8), 1319–1330.
[114] Harcombe, H., Samaranayaka, A., and Derrett, S. (2016) Predictors of Reduced Frequency of Physical Activity 3 Months After Injury: Findings From the Prospective Outcomes of Injury Study. *Physical Therapy*. 96 (12), 1885–1895.
[115] Grogan, B.F., Hsu, J.R., and Skeletal Trauma Research Consortium (2011) Volumetric muscle loss. *The Journal of the American Academy of Orthopaedic Surgeons*. 19 Suppl 1 S35-37.
[116] Greising, S.M., Warren, G.L., Southern, W.M., Nichenko, A.S., Qualls, A.E., Corona, B.T., et al. (2018) Early rehabilitation for volumetric muscle loss injury augments endogenous regenerative aspects of muscle strength and oxidative capacity. *BMC Musculoskeletal Disorders*. 19 (1), 173.
[117] Lusk, G. (1917) The elements of the science of nutrition,. 3d ed., reset. Philadelphia, .
[118] Seligman, A., Heymann, H., and Barnett, R. (1954) The histochemical demonstration of alkaline phosphatase activity with indoxyl phosphate. 2 441–442.
[119] Allen, D.L., Harrison, B.C., Maass, A., Bell, M.L., Byrnes, W.C., and Leinwand, L.A. (2001) Cardiac and skeletal muscle adaptations to voluntary wheel running in the mouse. *Journal of Applied Physiology (Bethesda, Md.: 1985)*. 90 (5), 1900–1908.
[120] Punsoni, M., Mangray, S., Lombardo, K.A., Heath, N., Stopa, E.G., and Yakirevich, E. (2017) Succinate Dehydrogenase B (SDHB) Immunohistochemistry for the Evaluation of Muscle Biopsies. *Applied Immunohistochemistry & Molecular Morphology: AIMM*. 25 (9), 645–650.
[121] Schiaffino, S., Gorza, L., Sartore, S., Saggin, L., Ausoni, S., Vianello, M., et al. (1989) Three myosin heavy chain isoforms in type 2 skeletal muscle fibres. *Journal of Muscle Research and Cell Motility*. 10 (3), 197–205.
[122] Greising, S.M., Mantilla, C.B., Gorman, B.A., Ermilov, L.G., and Sieck, G.C. (2013) Diaphragm muscle sarcopenia in aging mice. *Experimental Gerontology*. 48 (9), 881–887.
[123] Greising, S.M., Medina-Martínez, J.S., Vasdev, A.K., Sieck, G.C., and Mantilla, C.B. (2015) Analysis of muscle fiber clustering in the diaphragm muscle of sarcopenic mice. *Muscle & Nerve*. 52 (1), 76–82.
[124] Schneider, C.A., Rasband, W.S., and Eliceiri, K.W. (2012) NIH Image to ImageJ: 25 years of image analysis. *Nature Methods*. 9 (7), 671–675.

[125] Muoio, D.M. (2014) Metabolic Inflexibility: When Mitochondrial Indecision Leads to Metabolic Gridlock. *Cell*. 159 (6), 1253–1262.
[126] Greising, S.M., Corona, B.T., McGann, C., Frankum, J.K., and Warren, G.L. (2019) Therapeutic Approaches for Volumetric Muscle Loss Injury: A Systematic Review and Meta-Analysis. *Tissue Engineering Part B: Reviews*.
[127] Hoffman, D.B., Raymond-Pope, C.J., Sorensen, J.R., Corona, B.T., and Greising, S.M. (2021) Temporal changes in the muscle extracellular matrix due to volumetric muscle loss injury. *Connective Tissue Research*.
[128] Ibáñez-Fonseca, A., Santiago Maniega, S., Gorbenko Del Blanco, D., Catalán Bernardos, B., Vega Castrillo, A., Álvarez Barcia, Á.J., et al. (2020) Elastin-Like Recombinamer Hydrogels for Improved Skeletal Muscle Healing Through Modulation of Macrophage Polarization. *Frontiers in Bioengineering and Biotechnology*. 8 413.
[129] Adler, J. and Malone, D. (2012) Early Mobilization in the Intensive Care Unit: A Systematic Review. *Cardiopulmonary Physical Therapy Journal*. 23 (1), 5–13.
[130] Clark, D.E., Lowman, J.D., Griffin, R.L., Matthews, H.M., and Reiff, D.A. (2013) Effectiveness of an Early Mobilization Protocol in a Trauma and Burns Intensive Care Unit: A Retrospective Cohort Study. *Physical Therapy*. 93 (2), 186–196.